A COMPARISON OF LEAST-SQUARES FINITE ELEMENT MODELS WITH THE CONVENTIONAL FINITE ELEMENT MODELS OF PROBLEMS IN HEAT TRANSFER AND FLUID MECHANICS

A Thesis

by

NELLIE RAJAROVA

Submitted to the Office of Graduate Studies of
Texas A&M University
in partial fulfillment of the requirements for the degree of

MASTER OF SCIENCE

May 2009

Major Subject: Mechanical Engineering

A COMPARISON OF LEAST-SQUARES FINITE ELEMENT MODELS WITH THE CONVENTIONAL FINITE ELEMENT MODELS OF PROBLEMS IN HEAT TRANSFER AND FLUID MECHANICS

A Thesis

by

NELLIE RAJAROVA

Submitted to the Office of Graduate Studies of
Texas A&M University
in partial fulfillment of the requirements for the degree of

MASTER OF SCIENCE

Approved by:

Chair of Committee,	J.N.Reddy
Committee Members,	Xin-Lin Gao
	Jose Roesset
Head of Department,	Dennis O'Neal

May 2009

Major Subject: Mechanical Engineering

ABSTRACT

A Comparison of Least-Squares Finite Element Models with the Conventional Finite Element Models of Problems in Heat Transfer and Fluid Mechanics.

(May 2009)

Nellie Rajarova, B. Tech., National Institute of Technology, Rourkela

Chair of Advisory Committee: Dr. J. N. Reddy

In this thesis, least-squares based finite element models (LSFEM) for the Poisson equation and Navier-Stokes equation are presented. The least-squares method is simple, general and reliable. Least-squares formulations offer several computational and theoretical advantages. The resulting coefficient matrix is symmetric and positive-definite. Using these formulations, the choice of approximating space is not subject to any compatibility condition.

The Poisson equation is cast as a set of first order equations involving gradient of the primary variable as auxiliary variables for the mixed least-square finite element model. Equal order C^0 continuous approximation functions is used for primary and auxiliary variables. Least-squares principle was directly applied to develop another model which requires C^1continous approximation functions for the primary variable. Each developed model is compared with the conventional model to verify its performance.

Penalty based least-squares formulation was implemented to develop a finite element for the Navier Stokes equations. The continuity equation is treated as a constraint on the velocity field and the constraint is enforced using the penalty method. Velocity gradients are introduced as auxiliary variables to get the first order equivalent system. Both the primary and auxiliary variables are interpolated using equal order C^0 continuous, *p*-version approximation functions. Numerical examples are presented to demonstrate the convergence characteristics and accuracy of the method.

DEDICATION

To my Parents and God for their love and belief in me

ACKNOWLEDGEMENTS

I would like to thank my committee chair, Dr. J.N.Reddy for his guidance and support throughout the course of this research. His enthusiasm in research motivated me all the time. Thanks also go to my family and friends for their support.

I would like to thank Dr. Jose Roesset and Dr. Xin-Lin Gao, for their time and suggestions.

TABLE OF CONTENTS

		Page
ABSTRACT		iii
DEDICATION		v
ACKNOWLEDGEMENTS		vi
TABLE OF CONTENTS		vii
LIST OF FIGURES		ix
CHAPTER		
I	INTRODUCTION	1
	1.1. Background	1
	1.2. Development of Mathematical Models	6
	1.3. Numerical Methods	7
	1.4. Review of Weighted-Residual Methods	8
	1.4.1. Review of Galerkin's Methods	9
	1.4.2. The Least-Squares Method	10
II	FINITE ELEMENT MODELS FOR POISSON EQUATION	11
	2.1. Procedure for the Poisson Equation	12
	2.2. Conventional Weak Form Model (Model =1)	13
	2.2.1. Problem Statement	13
	2.2.2. Finite Element Model	15
	2.3. Mixed Least-Squares Model (Model=2)	16
	2.3.1. Problem Statement	16
	2.3.2. Finite Element Model	18
	2.4. Least-Squares Finite Element Model (Model=3)	22
	2.4.1. Problem Statement	22
	2.4.2. Finite Element Model	23
	2.5. Two Dimensional Lagrange Type Finite Element	24
	2.6. Hermite Cubic Type Finite Elements	25
	2.6.1. Non Conforming Rectangular Element	25
	2.6.2. Conforming Rectangular Element	27
	2.7. Numerical Results	28

CHAPTER Page

2.7.1. Numerical Example 1 28
2.7.1.1. Numerical Results for Model 1 29
2.7.1.2. Numerical Results for Model 2 32
2.7.1.3. Numerical Results for Model 3 34
2.7.2. Numerical Example 2 37
2.7.2.1. Numerical Results for Model 1 38
2.7.2.2. Numerical Results for Model 2 40

III FINITE ELEMENT MODELS FOR NAVIER-STOKES EQUATION 43

3.1. Incompressible Navier-Stokes Equations 43
3.1.1. Governing Equations 43
3.1.1.1. Conservation of Mass.................................. 44
3.1.1.2. Conservation of Linear Momentum 45
3.1.1.3. Conservation of Angular Momentum 45
3.1.1.4. Constitutive Equations 46
3.2. Conventional Mixed Model 47
3.3. Reduced Integration Penalty Model....................................... 49
3.4. Least-Squares Finite Element Model (Velocity Gradient Based).. 49
3.4.1. Finite Element Model for Navier-Stokes............... 51
3.4.2. Nonlinear Equation Solving Procedures................ 59
3.4.2.1. Direct Iteration Method................................ 58
3.4.3. Numerical Results... 61

IV CONCLUSIONS.. 66

REFERENCES... 68

VITA 72

LIST OF FIGURES

FIGURE Page

1.1. A spring mass system 6

2.1. Schematic showing the domain and the boundary 12

2.2. A Non confirming rectangular element.. 26

2.3. A Confirming rectangular element.. 28

2.4. Domain of the Poisson equation for problem in Example 1 29

2.5. Comparison of model1solution with exact solution for 2x2 mesh ,p=2 30

2.6. Comparison of model1solution with exact solution for 2x2 mesh ,p=4 30

2.7. Comparison of model1solution with exact solution for 2x2 mesh ,p=6 31

2.8. Comparison of model1solution with exact solution for 2x2 mesh ,p=8 31

2.9. Comparison of mixed LSFEM solution with exact solution
for 2x2 mesh, p=2.. 32

2.10. Comparison of mixed LSFEM solution with exact solution
for 2x2 mesh, p=4.. 32

2.11. Comparison of mixed LSFEM solution with exact solution
for 2x2 mesh, p=6.. 33

2.12. Comparison of mixed LSFEM solution with exact solution
for 2x2 mesh, p=8.. 33

2.13. Comparison of LSFEM solution with exact solution for 4x4 mesh................ 34

FIGURE Page

2.14. Comparison of LSFEM solution with exact solution for 6x6 mesh................ 35

2.15. Comparison of LSFEM solution with exact solution for 8x8 mesh................ 35

2.16. Comparison of LSFEM solution with exact solution for 15x15 mesh............ 36

2.17. Comparison of LSFEM solution with exact solution for 20x20 mesh............ 36

2.18. Domain of the Poisson equation for problem in Example 2 37

2.19. Comparison of model1 solution with series solution for 2x2 mesh,p=2.......... 38

2.20. Comparison of model1 solution with series solution for 2x2 mesh,p=4.......... 38

2.21. Comparison of model1 solution with series solution for 2x2 mesh,p=6.......... 39

2.22. Comparison of model1 solution with series solution for 2x2 mesh,p=8.......... 39

2.23. Comparison of mixed LSFEM solution with exact solution for 2x2 mesh, p=2.. 40

2.24. Comparison of mixed LSFEM solution with series solution for 2x2 mesh, p=4.. 41

2.25. Comparison of mixed LSFEM solution with series solution for 2x2 mesh, p=6.. 41

2.26. Comparison of mixed LSFEM solution with series solution for 2x2 mesh, p=8.. 42

3.1. A computer flow chart for the nonlinear finite element analysis...................... 60

3.2. Schematic of driven cavity problem.. 61

3.3. Finite element model of driven cavity... 61

3.4(a). Plots of u(x=0.5,y) at Re=100.. 62

3.4(b). Plots of u(x=0.5,y) at Re=400 62

FIGURE Page

3.4(c). Plots of u(x=0.5,y) at Re=1000.. 63

3.5(a). Plots of v(x=0.5,y) at Re=100.. 63

3.5(b). Plots of v(x=0.5,y) at Re=400 64

3.5(c). Plots of v(x=0.5,y) at Re=1000.. 64

CHAPTER I

INTRODUCTION

1.1. Background

In many of the scientific and engineering studies we have to deal with problems related to fluid mechanics and heat transfer. The main interest is to predict, understand and control complex fluid and thermal systems. The finite element method, despite being a powerful computational technique for the solution of differential and integral equations, has enjoyed great success in solid mechanics and heat conduction applications. It still has not achieved the same level of success in the field of fluid dynamics. Finite difference or finite volume techniques are widely used in the area of computational fluid dynamics (CFD). The main reason is that the finite element method involves considerable formulative effort. However, it is gaining popularity in CFD because of its generality of application to geometrically complex problems and multi-physics problems. The finite difference method (FDM), finite volume method (FVM), finite element method (FEM) [1], and boundary element method (BEM) [2] have been used to solve system of partial differential equation. When it comes to domains with complex geometries, the power of the FEM becomes more evident. By introducing a

---

This thesis follows the style of Computer Methods in Applied Mechanics and Engineering.

little more complexity in formulating the finite element model, many practical and useful multi-physics problems could be solved.

A large number of methods have been proposed for the numerical solution of the Navier-Stokes equations governing flows of viscous incompressible fluids. The Navier-Stokes equations can be expressed in terms of primitive variables (e.g., velocities and pressure) and auxiliary variables (e.g., velocity gradients, vorticity, stresses and stream function). The model will depend on the variables as well as the finite element method used. The common methods used are Galerkin, least-squares, collocation etc. Using the weighted-residual formulation with different choice of the weighted function results in various models. The conventional model is the one involving velocity, pressure as the primary variables (known as pressure-velocity formulation).

The biggest problem faced while using standard weak form Galerkin finite element model of multivariable problems is the use of compatible approximation spaces for the field variables (e.g., velocity and pressure). When the equations are nonlinear, the coefficient matrix is non-symmetric and thereby increasing computational cost. In the past few years finite element models based on least-squares variational principles have gained substantial interest [1, 3]. The formulation using *p* version least-squares method is more general than Galerkin-based methods. For problems related to fluid dynamics and convective heat transfer, the least-squares finite element method (LSFEM) has been advocated as a unified method [4].

The criteria desirable in a variational method suggested by Becker [5] include the following.

i. The procedure should minimize error in some sense.

ii. The integrand of the functional should be definite (admit values of one sign only).

iii. The procedure should be able to treat initial value problems.

Becker observed that LSFEM satisfies all the above criteria. LSFEM has been used widely applied to stokes flow [6], boundary layer flow [7], gas dynamics [8], inviscid compressible flow [9], convection-diffusion [10] and phase change problems [11]. Systems of elliptic [12], hyperbolic [13] and mixed [14] partial differential equations have been solved using LSFEM.

The most notable outcome of this method is that equal order interpolation functions can be used for all field variables, but with higher-order polynomial expansions, and hence circumventing the inf-sup condition of Ladyzhenskaya-Babuska-Brezzi (LBB). In the least-squares formulations, even the essential boundary conditions can be imposed in weak sense [3]. The resulting system of algebraic equations yield symmetric, positive-definite coefficient matrix and facilitate the use of robust iterative solvers.

Direct application of least-squares principles to develop finite element models for 2mth-order differential operators require that the finite element space be spanned by functions that belong to the Hilbert space H^{2m}, in contrast to weak form Galerkin models which require only H^{m} regularity. In deriving the Galerkin model the differentiability of the operators is weakened due to integration by parts step, this allows lower smoothness requirement. The higher smoothness requirement is the major drawback of least-square based formulation.

Earlier, least squares principles were directly applied to Navier-Stokes equations, requiring the polynomial approximations to be C^1 continuous. Due to this stringent constraint on the approximation space, the method failed to gain popularity during earlier days. To allow the use of practical C^0 element expansions in the least-squares finite element model, the governing equations have to be first cast into an equivalent first order system. This requires the introduction of additional independent variables at every node, resulting in an increase in cost. However, the auxiliary variables may be beneficial as they might represent physically meaningful variables. Certain variables that are of practical importance can be made independent variables, instead of post computing, e.g. strains, stresses or fluxes.

The *p*-version is supposed to have superior convergence characteristics than *h*-version [15]. Jiang and Sonnad [16] applied *p*-version least square finite element formulation to Navier-Stokes velocity-pressure-vorticity based first-order system. Detailed numerical results were however presented by Pontaza and Reddy [1].They also studied the velocity-gradient based first order system. K.S Surana and coworkers [17] presented *p* version approximation clubbed with least-square formulation based on minimization of the least square functional derived using non linear partial differential equations without linearization. The model was based on stress based first order system.

In this study two different equations were considered: (1) problems described by the Poisson equation and (2) the Navier-Stokes equations governing flows of viscous incompressible fluids. The Poisson equation considered here is of the form $\nabla^2\phi = f$ .It arises in many fields of engineering, for example, heat transfer, magnetic flux density

[3], charge density [18], computer vision [2], etc. The formulation for Navier-Stokes presented here is penalty based least-squares finite element formulation for velocity gradient based first order system. Iterative penalty method proposed by Gunzberger [19] was implemented. The formulation uses *p*-approximation functions based on Lagrange interpolating polynomials and includes velocity gradients as variables. Least squares formulation result in a minimization problem and the choice of the approximation functions for the field variables is not subjected to the LBB condition. Locking is not experienced when higher order element expansions are used for the field variables.

In this study we try to investigate the performance of various finite element models based on several weighted-residual formulations applied to problems in fluid dynamics and heat transfer. We shall investigate the merits and demerits of the different models and the accuracy with which they can predict the field variables. They will be based on the weak form Galerkin formulations and least-squares formulations of at least two sets of equations of the same physical problem.

Selection of an appropriate formulation of the governing equations to develop the discrete system of algebraic equations (called a *finite element model*) is necessary to be able to apply this method to any fluid dynamics or heat transfer problem. Most finite element formulations are based on variational methods (i.e., methods based on a functional that is equivalent to the governing equations) or weighted-residual methods (i.e., weighted-integral statements of the governing equations). However, very few fluid dynamic (or heat transfer) problems can be expressed in a variational setting. Alternative to the variational method is use of the weighted-residual methods, which include subdomain method, collocation method, Galerkin method, Petrov-Galerkin method, and least-squares method. In addition to the method of discretization, the choice of equations (or field variables) used to describe the physics yield different finite element models. In other words, the same physical problem can be cast in alternative forms by selecting the field variables. Thus, there are numerous finite element models of a physical problem depending on the choice of the method of discretization and variables.

1.2. Development of Mathematical Models

A mathematical model analytically expresses a physical phenomenon. It describes the system in terms of variables. The models are based on fundamental laws of physics like conservation of mass, conservation of linear momentum, conservation of angular momentum, conservation of energy and constitutive equations.

Consider the system shown in Fig. 1.1.,

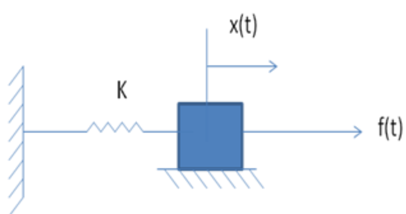

Fig. 1.1. A spring mass system

where, K is the spring constant, x(t) is the displacement and f is force. Applying conservation of momentum to the system, the mathematical model is obtained.

$$F = \frac{d}{dt}(mv), \tag{1.1}$$

If m is constant, the above equation is written as $F = m\frac{d}{dt}(v) = ma = m\frac{d^2x}{dt^2}$

So the mathematical model is given by,

$$m\frac{d^2x}{dt^2} + kx = f(t), \tag{1.2}$$

The laws and axioms governing the processes are usually complex differential equations posed on a geometrically complicated domain. It is not always possible to find out analytical solution to all the problems. Numerical methods and high computational abilities of present generation computers have made it possible to find an approximate solution to these problems. The finite element method is a numerical method that can be used to analyze practical engineering problems.

1.3. Numerical Methods

Numerical methods help in getting an approximate solution to a mathematical model by transforming the differential equations into a set of algebraic equations. Many numerical methods have been developed to solve differential equations. For example finite difference method, finite volume method and classical variational methods are some of the numerical methods extensively used in finding an approximate solution. The classical variational methods (e.g. Ritz, Galerkin, Petrov-Galerkin, collocation and least-squares, etc.) are powerful techniques that provide globally continuous solutions. The major disadvantage of classical variational methods is the difficulty in constructing the approximate functions for arbitrary domains.

1.4. Review of Weighted-Residual Methods

Weighted-residual methods are those in which we seek approximate solutions using a weighted-integral statement of equations [20]

Consider the operator equation

$$A(u) - f = 0 \quad in \quad \Omega, \tag{1.3}$$

subjected to boundary conditions

$$B(u) = g \quad on \quad \Gamma, \tag{1.4}$$

where, A is a differential operator (linear or nonlinear), f is the source term and B is the boundary operator associated with A. The approximate solution u is of the form

$$u \approx u_n = \sum_{j=1}^{n} c_j \phi_j(\mathbf{x}) + \phi_o(\mathbf{x}), \tag{1.5}$$

As u_n is an approximate, on substituting it in equation (1.3), a residual statement is obtained. The weighted-residual statement of equation (1.3) is stated as

$$0 = \int_{\Omega^e} w\left[A(u_n) - f\right]\mathrm{d}\mathbf{x} \tag{1.6}$$

$$0 = \int_{\Omega^e} \psi_i \left[R_n\left(x, c_j, \phi_j, f\right)\right]\mathrm{d}\mathbf{x} \qquad i = 1,2,3......n \tag{1.7}$$

$$R_n \equiv A\left(\sum_{j=1}^{n} c_j \phi_j + \phi_0\right) - f \neq 0 \tag{1.8}$$

ψ_i, ϕ_i are the weight functions, approximation functions respectively. Equation (1.7) provides n linearly independent equations for the determination of the parameter c_j. Depending on the choice of the weight function, we have various cases of the weighted-residual method. Some of them are,

The Petrov-Galerkin method $\psi_i \neq \phi_i$

Galerkin's method: $\psi_i = \phi_i$

Least-squares method: $\psi_i = \dfrac{\partial R}{\partial c_i} = A(\phi_i)$

Collocation method: $\psi_i = \delta(x - x_i)$

Subdomain method: $\psi_i = 1, \quad \Omega = \bigcup_{i=1}^{n} \Omega_i, \quad \int_{\Omega_i} \left[R\left(x, c_j, \phi_j, f\right)\right] d\mathbf{x} = 0$

1.4.1. Review of Galerkin's Methods

Consider the operator equation (1.3), the weight functions are chosen from the same family of approximating functions. The algebraic equations for this approximation is

$$\lfloor A_{ij} \rfloor \{c_j\} - F_i = 0 \tag{1.9}$$

$$A_{ij} = \int_{\Omega^e} \phi_i A(\phi_j) d\tilde{x} \qquad F_i = \int_{\Omega^e} \phi_i [f - A(\phi_0)] d\tilde{x} \tag{1.10}$$

1.4.2. The Least-Squares Method

The coefficients c_j are determined by minimizing the integral of the square of the residual.

Minimize

$$I(c_i) = \int_{\Omega} (R_1{}^2 + R_2{}^2 + \ldots\ldots R_n{}^2) dx \tag{1.11}$$

$$\delta I = 0 = \frac{\partial}{\partial c_i} \int_{\Omega} R^2(x, c_j) d\tilde{x} \tag{1.12}$$

This shows that the weight function is $\psi_i = \dfrac{\partial R}{\partial c_i} = A(\phi_i)$. The least-squares method results in positive definiteness of the coefficient matrix.

CHAPTER II

FINITE ELEMENT MODELS FOR POISSON EQUATION

Poisson equation in two dimensions was considered. Finite element models were obtained using three different formulations. The Poisson equation can be stated as finding the solution $u(\mathbf{x})$ that will satisfy the following equations:

$$-\nabla^2 u + cu = f \; in \quad \Omega, \tag{2.1}$$

$$u = u^p \; on \quad \Gamma_u, \tag{2.2}$$

$$\hat{n}.\nabla u = q_n^s \; on \quad \Gamma_q, \tag{2.3}$$

where, Ω is an open bounded region in $\Re^n$ and $\Gamma = \Gamma_u \cup \Gamma_q$ and $\Gamma_u \cap \Gamma_q = \emptyset$ as shown in Fig.2.1. Value of n represents the number of space dimensions. If n=2, then it represents a two-dimensional space and represents three-dimensional space if n=3. Γ is the boundary of the domain Ω. Equations (2.2) and (2.3) explain the boundary conditions. u^p is the prescribed value of u on Γ_u, and q_n^s is the prescribed normal flux on the boundary Γ_q. $\hat{n}$ is the outward unit normal on Γ.

The models are based on the weak form Galerkin method and least-squares principles. Different numerical problems were solved using the different models, implementing both *p*-refinement as well as *h*-refinement. *h*-refinement is achieved by using more of the same kind of elements, whereas *p*-refinement is implemented by using higher order elements. For instance we are discretizing our domain into NxN elements, each element approximation is of order '*p*'. For *h*-refinement we will have more than NxN elements and for *p*-refinement we will still have NxN elements but the order will be greater than '*p*'. Practical C^0 element expansion and C^1 element expansion were used and the results were compared using the resulting finite element model.

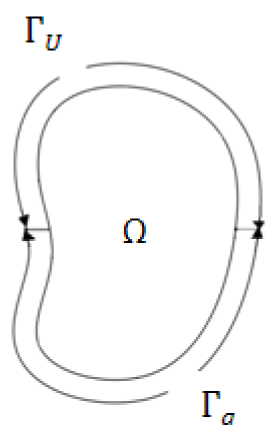

Fig.2.1. Schematic showing the domain and the boundary

2.1 Procedure for the Poisson Equation

Consider the two dimensional Poisson equation in component form,

$$-\frac{\partial}{\partial x}\left(a_{xx}\frac{\partial u}{\partial x}\right)-\frac{\partial}{\partial y}\left(a_{yy}\frac{\partial u}{\partial y}\right)+cu-f=0 \;\; in \;\; \Omega, \tag{2.4}$$

$$a_{xx}\left(\frac{\partial u}{\partial x}\right)n_x - a_{yy}\left(\frac{\partial u}{\partial y}\right)n_y - q = 0, \quad on \quad \Gamma \tag{2.5}$$

By using eqns. (1a) and (1b) we shall get the conventional formulation involving $u(x, y)$ as the field variable. By introducing auxiliary variables, we obtain the mixed least- squares model. The different formulations are listed as models. The three different models presented are

(1) Model 1: Weak-form finite element model based on eqns. (2.4) and (2.5).

(2) Model 2: Mixed least-square formulation based on alternative sets of equations.

(3) Model 3: Least-squares finite element model based on eqns. (2.4) and (2.5).

2.2. Conventional Weak Form Model (Model =1)

2.2.1. Problem Statement

Consider the two dimensional Poisson equation over a element domain Ω^e,

$$-\frac{\partial}{\partial x}\left(a_{xx}\frac{\partial u}{\partial x}\right)-\frac{\partial}{\partial y}\left(a_{yy}\frac{\partial u}{\partial y}\right)+cu-f=0, in \quad \Omega \tag{2.6}$$

$$a_{xx}\left(\frac{\partial u}{\partial x}\right)n_x+a_{yy}\left(\frac{\partial u}{\partial y}\right)n_y-q=0, \; on \;\; \Gamma \tag{2.7}$$

Multiplying the equation with a weight function $w \in H^1$, and integrating the resulting equation over the whole domain Ω^e, equation (2.8) is obtained.

$$\int_{\Omega^e} w\left[-\frac{\partial}{\partial x}\left(a_{xx}\frac{\partial u}{\partial x}\right)-\frac{\partial}{\partial y}\left(a_{yy}\frac{\partial u}{\partial y}\right)+cu-f\right]dxdy=0, \tag{2.8}$$

To get the weak form, the first two terms have to be integrated by parts to equally distribute the differentiation on *u* and *w*.

$$\int_{\Omega^e}\left[\frac{\partial w}{\partial x}\left(a_{xx}\frac{\partial u}{\partial x}\right)+\frac{\partial w}{\partial y}\left(a_{yy}\frac{\partial u}{\partial y}\right)+cwu-fw\right]dxdy \tag{2.9}$$
$$-\oint_{\Gamma^e} w\left[a_{xx}\left(\frac{\partial u}{\partial x}\right)n_x+a_{yy}\left(\frac{\partial u}{\partial y}\right)n_y\right]ds=0$$

Using equation (2.9) we write the weak form as

$$\int_{\Omega^e}\left[\frac{\partial w}{\partial x}\left(a_{xx}\frac{\partial u}{\partial x}\right)+\frac{\partial w}{\partial y}\left(a_{yy}\frac{\partial u}{\partial y}\right)+cwu-fw\right]dxdy \tag{2.10}$$
$$-\oint_{\Gamma^e} wqds=0$$

The bilinear form is written as

$$B^e(w,u)=l^e(w), \tag{2.11}$$

where,

$$B^e(w,u)=\int_{\Omega^e}\left[\frac{\partial w}{\partial x}\left(a_{xx}\frac{\partial u}{\partial x}\right)+\frac{\partial w}{\partial y}\left(a_{yy}\frac{\partial u}{\partial y}\right)+cwu\right]dxdy \tag{2.12}$$

$$l^e(w)=\int_{\Omega^e} fwdxdy-\oint_{\Gamma^e} wqds$$

So the variational problem can be stated as finding $u(x,y)\in\mathbf{X}$ such that $\forall(w)\in\mathbf{X}$

$$B^e(w,u)=l^e(w),$$

where, $\mathbf{X}$ is the solution space denoted by

$$\mathbf{X}=\left\{(u,w)\in H^1(\Omega)\times H^1(\Omega)\middle| u|_{\Gamma_u}=u^p\right\}$$

As the bilinear form is symmetric in its arguments *w* and *u*, we can form the quadratic functional

$$I^e(w) = \frac{1}{2}B^e(w,w) - l^e(w) \tag{2.13}$$
$$= \frac{1}{2}\int_{\Omega^e}\left[a_{xx}\left(\frac{\partial u}{\partial x}\right)^2 + a_{yy}\left(\frac{\partial u}{\partial y}\right)^2 + cu^2\right]dxdy - \int_{\Omega^e} fudxdy - \oint_{\Gamma^e} quds$$

Minimizing the quadratic functional yields the equation $\delta I^e = 0$. This is equivalent to equations (2.5), (2.6) and these are the Euler-Lagrange equations for the minimization problem.

2.2.2. Finite Element Model

The finite element formulation allows us to use Lagrange family of interpolation function as the primarily variable is just *u* and not its derivatives. The field variable *u* is approximated as,

$$u(x,y) \approx u_h(x,y) = \sum_{j=1}^{N} u_j^e \psi_j^e(x,y) \tag{2.14}$$

The following finite element model was obtained by substituting equation (2.14) in the weak form (2.9).

$$\sum_{j=1}^{N}\left\{\int_{\Omega^e}\left[\frac{\partial \psi_i}{\partial x}\left(a_{xx}\frac{\partial \psi_j}{\partial x}\right) + \frac{\partial \psi_i}{\partial y}\left(a_{yy}\frac{\partial \psi_j}{\partial y}\right) + c\psi_i\psi_j\right]dxdy\right\}u_j - \int_{\Omega^e} f\psi_i - \oint_{\Gamma^e}\psi_i qds = 0$$

(2.15)

In matrix form equation (2.15) can be written as,

$$\left[K^e\right]\left\{u^e\right\}=\left\{F^e\right\} \tag{2.16}$$

where,

$$K^e = K_{ij}^e = \int_{\Omega^e}\left[\frac{\partial\psi_i}{\partial x}\left(a_{xx}\frac{\partial\psi_j}{\partial x}\right)+\frac{\partial\psi_i}{\partial y}\left(a_{yy}\frac{\partial\psi_j}{\partial y}\right)+c\psi_i\psi_j\right]dxdy, \tag{2.17}$$

$$F^e = F_i^e = \int_{\Omega^e} f\psi_i + \oint_{\Gamma^e}\psi_i q ds \tag{2.18}$$

2.3. Mixed Least-Squares Model (Model =2)

2.3.1. Problem Statement

In this model, the Poisson problem is replaced with its first order equivalent. The problem can now be stated as finding $u(\mathbf{x})$ and $v(\mathbf{x})$ such that

$$-\nabla.\mathbf{v}+cu=f \ \ in \quad \Omega \tag{2.19}$$

$$\nabla u-\mathbf{v}=\mathbf{0} \ \ in \ \ \Omega \tag{2.20}$$

$$u=u^p \ \ on \ \ \Gamma_u, \tag{2..21}$$

$$\hat{\mathbf{n}}.\mathbf{v}=q_n^s \ \ on \ \ \Gamma_q, \tag{2.22}$$

where, **v** is a vector valued function with components v_x, v_y (two-dimensional space) being the fluxes of u defined in equation (2.20) .The L_2 least-square functional associated with the first order equivalent of the Poisson problem is

$$\mathrm{I}(u,v;f) = \frac{1}{2}\left(\left\| -\nabla.v + cu - f \right\|_0^2 + \left\| \nabla u - v \right\|_0^2\right) \tag{2.23}$$

Considering homogeneous boundary condition, the least-squares principle for functional (2.23) can be stated as

Find (u ,**v**) **ϵ X** such that $\forall(\psi,\phi)$ **ϵ X**

$$\mathrm{I}(u,v;f) \le \mathrm{I}(\psi,\phi;f), \tag{2.24}$$

Where **X** is the solution space denoted by

$$X = \left\{(u,v) \in H^1(\Omega) \times H^1(\Omega) \middle| u|_{\Gamma_u} = 0, \hat{n}.v|_{\Gamma_q} = 0\right\} \tag{2.25}$$

The variational problem is described as

Find $(u,v) \in \mathbf{X}$ such that $\forall(\psi,\phi) \in \mathbf{X}$

$$B((u,v),(\psi,\varphi)) = F(\psi,\varphi), \tag{2.26}$$

where**,**

$$B((u,v),(\psi,\varphi)) = \int_{\Omega^e} (-\nabla.v + cu)(-\nabla.\varphi + c\psi) d\Omega + \int_{\Omega^e} (\nabla u - v)(\nabla\psi - \varphi) d\Omega \tag{2.27}$$

and

$$F((\psi, \varphi)) = \int_{\Omega^e} f(-\nabla.\varphi + c\psi)d\Omega \quad (2.28)$$

2.3.2. Finite Element Model

Now we replace the Poisson problem with its first-order system equivalent. If we introduce the vector $v = (v_x, v_y)$, where v_x and v_y are the horizontal and vertical components of the velocity field, we obtain an alternative set of equations based on eqns. (1a) and (1b),

$$a_{xx}\left(\frac{\partial u}{\partial x}\right) + v_x = 0 \quad (2.29)$$

$$a_{yy}\left(\frac{\partial u}{\partial y}\right) + v_y = 0 \quad (2.30)$$

$$\frac{\partial v_x}{\partial x} + \frac{\partial v_y}{\partial y} + cu - f = 0 \quad (2.31)$$

$$v_x n_x + v_y n_y - q = 0 \quad (2.32)$$

The model based on the first order system equivalent will have $u(x, y), v_x(x, y)_x, v_y(x, y)$ as the field variables. It will be denoted as mixed model. Let u^h, v_x^h, v_y^h, represent the finite element approximation to the true solution u, v_x, v_y. To develop the least-squares finite element model, the residuals over a typical element Ω^e is given as,

$$I^e = \frac{1}{2}\int_{\Omega^e}\left(R_1^2 + R_2^2 + R_3^2\right)dxdy \tag{2.33}$$

where,

$$R_1 = \frac{\partial u^h}{\partial x} + \frac{v_x^h}{a_{xx}}, \qquad R_2 = \frac{\partial u^h}{\partial y} + \frac{v_y^h}{a_{yy}}, \qquad R_3 = \frac{\partial v_x^h}{\partial x} + \frac{\partial v_y^h}{\partial y} + cu^h - f \tag{2.34}$$

The functional associated with equations (2.33) is

$$I^e\left(u, v_{x,} v_y\right) = \int_{\Omega^e}\left[\left(\frac{\partial u^h}{\partial x} + \frac{v_x^h}{a_{xx}}\right)^2 + \left(\frac{\partial u^h}{\partial y} + \frac{v_y^h}{a_{yy}}\right)^2 + \left(\frac{\partial v_x^h}{\partial x} + \frac{\partial v_y^h}{\partial y} + cu^h - f\right)^2\right]dxdy \tag{2.35}$$

The primary variables were approximated by expansions of the form

$$u^h(x,y) = \sum_{i=1}^{N}\psi_i(x,y)u_i, \quad v_x^h(x,y) = \sum_{i=1}^{N}\psi_i(x,y)v_x^i, \quad v_y^h(x,y) = \sum_{i=1}^{N}\psi_i(x,y)v_y^i \tag{2.36}$$

The above least-squares functional was minimized with respect to the nodal values of velocities and velocity gradients

$$0 = \delta I^e\left(u, v_{x,} v_y\right) = \frac{\partial I^e}{\partial u^h}\delta u^h + \frac{\partial I^e}{\partial v_x^h}\delta v_x^h + \frac{\partial I^e}{\partial v_y^h}\delta v_y^h \equiv R^T\delta\Delta, \tag{2.37}$$

Equation (2.37) resulted in a set of three equations each over a typical element.

$$0 = \frac{\partial I^e}{\partial u^i} \equiv R_i^1 = \int_{\Omega^e}\left(R_1\frac{\partial R_1}{\partial u^i} + R_2\frac{\partial R_2}{\partial u^i} + R_3\frac{\partial R_3}{\partial u^i}\right)dxdy, \tag{2.38}$$

$$= \int_{\Omega^e}\left[\frac{\partial \Psi_i}{\partial x}\left(\frac{\partial u^h}{\partial x} + \frac{v_x^h}{a_{xx}}\right) + \frac{\partial \Psi_i}{\partial y}\left(\frac{\partial u^h}{\partial y} + \frac{v_y^h}{a_{yy}}\right) + c\psi_i\left(\frac{\partial v_x^h}{\partial x} + \frac{\partial v_y^h}{\partial y} + cu^h - f\right)\right]dxdy$$

$$0 = \frac{\partial I^e}{\partial v_x^i} \equiv R_i^2 = \int_{\Omega^e} \left(R_1 \frac{\partial R_1}{\partial v_x^i} + R_2 \frac{\partial R_2}{\partial v_x^i} + R_3 \frac{\partial R_3}{\partial v_x^i} \right) dxdy$$

$$= \int_{\Omega^e} \left[\frac{\Psi_i}{a_{xx}} \left(\frac{\partial u^h}{\partial x} + \frac{v_x^h}{a_{xx}} \right) + \frac{\partial \Psi_i}{\partial x} \left(\frac{\partial v_x^h}{\partial x} + \frac{\partial v_y^h}{\partial y} + cu^h - f \right) \right] dxdy \qquad (2.39)$$

$$0 = \frac{\partial I^e}{\partial v_y^i} \equiv R_i^3 = \int_{\Omega^e} \left(R_1 \frac{\partial R_1}{\partial v_y^i} + R_2 \frac{\partial R_2}{\partial v_y^i} + R_3 \frac{\partial R_3}{\partial v_y^i} \right) dxdy \qquad (2.40)$$

$$= \int_{\Omega^e} \left[\frac{\Psi_i}{a_{yy}} \left(\frac{\partial u^h}{\partial y} + \frac{v_y^h}{a_{yy}} \right) + \frac{\partial \Psi_i}{\partial y} \left(\frac{\partial v_x^h}{\partial x} + \frac{\partial v_y^h}{\partial y} + cu^h - f \right) \right] dxdy$$

The integral statements were written in matrix form and the following finite element model was obtained.

$$\begin{bmatrix} [K_{ij}^{11}] & [K_{ij}^{12}] & [K_{ij}^{13}] \\ [K_{ij}^{21}] & [K_{ij}^{22}] & [K_{ij}^{23}] \\ [K_{ij}^{31}] & [K_{ij}^{32}] & [K_{ij}^{33}] \end{bmatrix} \begin{Bmatrix} \{u\} \\ \{v_x\} \\ \{v_y\} \end{Bmatrix} = \begin{Bmatrix} \{F^1\} \\ \{F^2\} \\ \{F^3\} \end{Bmatrix} \qquad (2.41)$$

where,

$$K_{ij}^{11} = \int_{\Omega^e} \left[\frac{\partial \psi_i}{\partial x} \frac{\partial \psi_j}{\partial x} + \frac{\partial \psi_i}{\partial y} \frac{\partial \psi_j}{\partial y} + c^2 \psi_i \psi_j \right] dxdy$$

$$K_{ij}^{12} = \int_{\Omega^e} \left[\frac{1}{a_{xx}} \frac{\partial \Psi_i}{\partial x} \Psi_j + c\Psi_i \frac{\partial \Psi_j}{\partial x} \right] dxdy = \left[K_{ij}^{21} \right]^T \qquad (2.42)$$

$$K_{ij}^{13} = \int_{\Omega^e} \left[\frac{1}{a_{yy}} \frac{\partial \psi_i}{\partial y} \psi_j + c\psi_i \frac{\partial \psi_j}{\partial y} \right] dxdy = \left[K_{ij}^{31}\right]^T$$

$$K_{ij}^{22} = \int_{\Omega^e} \left[\frac{1}{a_{xx}{}^2} \psi_i \psi_j + \frac{\partial \psi_i}{\partial x} \frac{\partial \psi_j}{\partial x} \right] dxdy$$

$$K_{ij}^{23} = \int_{\Omega^e} \left[\frac{\partial \psi_i}{\partial x} \frac{\partial \psi_j}{\partial y} \right] dxdy = \left[K_{ij}^{32}\right]^T$$

$$K_{ij}^{33} = \int_{\Omega^e} \left[\frac{1}{a_{yy}{}^2} \psi_i \psi_j + \frac{\partial \psi_i}{\partial y} \frac{\partial \psi_j}{\partial y} \right] dxdy$$

$$F_i^1 = \int_{\Omega^e} \left[cf\psi_i \right] dxdy$$

$$F_i^2 = \int_{\Omega^e} \left[f \frac{\partial \psi_i}{\partial x} \right] dxdy$$

$$F_i^3 = \int_{\Omega^e} \left[f \frac{\partial \psi_i}{\partial y} \right] dxdy$$

The curl constraint $\nabla \times v = 0$ was added to ensure coercivity of the system [3].

Equations (2.38-2.40) were modified after including $R_4 = \frac{\partial v_x^h}{\partial y} - \frac{\partial v_y^h}{\partial x} = 0$ as follows

$$R_i^1 = \int_{\Omega^e} \left[\frac{\partial \Psi_i}{\partial x} \left(\frac{\partial u^h}{\partial x} + \frac{v_x^h}{a_{xx}} \right) + \frac{\partial \Psi_i}{\partial y} \left(\frac{\partial u^h}{\partial y} + \frac{v_y^h}{a_{yy}} \right) + c\psi_i \left(\frac{\partial v_x^h}{\partial x} + \frac{\partial v_y^h}{\partial y} + cu^h - f \right) \right] dxdy$$

$$R_i^2 = \int_{\Omega^e} \left[\frac{\Psi_i}{a_{xx}} \left(\frac{\partial u^h}{\partial x} + \frac{v_x^h}{a_{xx}} \right) + \frac{\partial \Psi_i}{\partial x} \left(\frac{\partial v_x^h}{\partial x} + \frac{\partial v_y^h}{\partial y} + cu^h - f \right) + \frac{\partial \psi_i}{\partial y} \left(\frac{\partial v_x^h}{\partial y} - \frac{\partial v_y^h}{\partial x} \right) \right] dxdy$$

$$R_i^3 = \int_{\Omega^e} \left[\frac{\Psi_i}{a_{yy}} \left(\frac{\partial u^h}{\partial y} + \frac{v_y^h}{a_{yy}} \right) + \frac{\partial \Psi_i}{\partial y} \left(\frac{\partial v_x^h}{\partial x} + \frac{\partial v_y^h}{\partial y} + cu^h - f \right) + \frac{\partial \psi_i}{\partial x} \left(\frac{\partial v_x^h}{\partial y} - \frac{\partial v_y^h}{\partial x} \right) \right] dxdy$$

The coefficients $\left[K_{ij}^{22}\right], \left[K_{ij}^{23}\right] and \left[K_{ij}^{33}\right]$ were only modified.

$$K_{ij}^{22} = \int_{\Omega^e} \left[\frac{1}{a_{xx}{}^2} \psi_i \psi_j + \frac{\partial \psi_i}{\partial x} \frac{\partial \psi_j}{\partial x} + \frac{\partial \psi_i}{\partial x} \frac{\partial \psi_j}{\partial x} \right] dxdy$$

$$K_{ij}^{23} = \int_{\Omega^e} \left[\frac{\partial \Psi_i}{\partial x} \frac{\partial \Psi_j}{\partial y} - \frac{\partial \Psi_i}{\partial y} \frac{\partial \Psi_j}{\partial x} \right] dxdy = \left[K_{ij}^{32}\right]^T \qquad (2.43)$$

$$K_{ij}^{33} = \int_{\Omega^e} \left[\frac{1}{a_{yy}{}^2} \psi_i \psi_j + \frac{\partial \psi_i}{\partial y} \frac{\partial \psi_j}{\partial y} + \frac{\partial \psi_i}{\partial x} \frac{\partial \psi_j}{\partial x} \right] dxdy$$

2.4. Least-Squares Finite Element Model (Model=3)

2.4.1. Problem Statement

This model is the least-square finite element model for equation (2.5). The least-squares functional associated with equation (2.5) over a typical element Ω^e is

$$I^e(u) = \int_{\Omega^e} \left[-\frac{\partial}{\partial x} \left(a_{xx} \frac{\partial u}{\partial x} \right) - \frac{\partial}{\partial y} \left(a_{yy} \frac{\partial u}{\partial y} \right) + cu - f \right]^2 dxdy \qquad (2.44)$$

The first variation of the least-squares functional was set to zero.

$$\delta I^e(u) = \int_{\Omega^e}\left[\frac{\partial}{\partial x}\left(a_{xx}\frac{\partial \delta u}{\partial x}\right)\frac{\partial}{\partial y}\left(a_{yy}\frac{\partial \delta u}{\partial y}\right) - c\delta u\right]\left[\frac{\partial}{\partial x}\left(a_{xx}\frac{\partial u}{\partial x}\right)\frac{\partial}{\partial y}\left(a_{yy}\frac{\partial u}{\partial y}\right) - cu + f\right]dxdy \tag{2.45}$$

2.4.2. Finite Element Model

The finite element approximation of the primary variable $u(x, y)$ is of the form

$$u(x, y) \approx u^h(x, y) = \sum_{j=1}^{m}\Delta_j^e \varphi_j^e(x, y) \tag{2.46}$$

where, $\varphi_j(x, y)$ are the Hermite cubic family of interpolation functions. Δ_j^e are the nodal values of the nodal variables $\left(u, \frac{\partial u}{\partial x}, \frac{\partial u}{\partial y}, \frac{\partial^2 u}{\partial x \partial y}\right)$.

The finite element model in matrix form is written as

$$\left[K^e\right]\left\{\Delta^e\right\} = \left\{F^e\right\}$$

where,

$$K_{ij}^e = \int_{\Omega^e}\left[\frac{\partial}{\partial x}\left(a_{xx}\frac{\partial \varphi_i}{\partial x}\right)\frac{\partial}{\partial y}\left(a_{yy}\frac{\partial \varphi_i}{\partial y}\right) - c\varphi_i\right]\left[\frac{\partial}{\partial x}\left(a_{xx}\frac{\partial \varphi_j}{\partial x}\right)\frac{\partial}{\partial y}\left(a_{yy}\frac{\partial \varphi_j}{\partial y}\right) - c\varphi_j\right]dxdy \tag{2.47}$$

$$F_i^e = -\int_{\Omega^e}\left[\frac{\partial}{\partial x}\left(a_{xx}\frac{\partial \varphi_i}{\partial x}\right) + \frac{\partial}{\partial y}\left(a_{yy}\frac{\partial \varphi_i}{\partial y}\right) - c\varphi_i\right]f dxdy$$

2.5. Two Dimensional Lagrange Type Finite Element

For model (1) and (2) Lagrange type interpolation functions for rectangular elements were used as approximations for the primary variables. They are derived from the corresponding one-dimensional Lagrange interpolation function by taking the tensor product of the x direction (one-dimensional) interpolation function with the y direction (one-dimensional) interpolation functions. The *p*th order interpolation function is given by

$$\begin{bmatrix} \Psi_1 & \Psi_{p+2} & \cdots & \Psi_k \\ \Psi_2 & & & \\ \vdots & \ddots & & \vdots \\ \Psi_p & & \ddots & \\ \Psi_{p+1} & \Psi_{2p+2} & & \Psi_n \end{bmatrix} = \begin{Bmatrix} f_1 \\ f_2 \\ \vdots \\ f_{p+1} \end{Bmatrix} \begin{Bmatrix} g_1 \\ g_2 \\ \vdots \\ g_{p+1} \end{Bmatrix}^T \qquad (2.48)$$

$$k = p(p+1)+1, \qquad n = (p+1)(p+1)$$

where $f_i(x)$ and $g_i(y)$ are the *p*th order interpolants in x and y, respectively.

$$f_i(\xi) = \frac{(\xi - \xi_1)(\xi - \xi_2)\ldots(\xi - \xi_{i-1})(\xi - \xi_{i+1})\ldots(\xi - \xi_{p+1})}{(\xi_i - \xi_1)(\xi_i - \xi_2)\ldots(\xi_i - \xi_{i-1})(\xi_i - \xi_{i+1})\ldots(\xi_i - \xi_{p+1})} \qquad (2.49)$$

The *p*th order interpolation polynomial $f_i(\xi)$ vanishes at points ξ_1, ξ_2, …. ξ_{i-1}, ξ_{i+1}, ….., ξ_{p+1}. ξ_i is the ξ coordinate of node i.

Similarly,

$$g_i(\eta) = \frac{(\eta - \eta_1)(\eta - \eta_2)\ldots(\eta - \eta_{i-1})(\eta - \eta_{i+1})\ldots(\eta - \eta_{p+1})}{(\eta_i - \eta_1)(\eta_i - \eta_2)\ldots(\eta_i - \eta_{i-1})(\eta_i - \eta_{i+1})\ldots(\eta_i - \eta_{p+1})} \tag{2.50}$$

η_i is the η coordinate of node i. Constructing the interpolation function is convenient when element coordinates (x, y) are expressed in local coordinates (ξ, η). Gauss-Derivation of the Lagrange family of interpolation functions in terms of natural coordinates (ξ, η) is based on the following interpolation property of the approximation functions.

$$\psi_i(\xi_j) = \begin{cases} 1 \mathit{if}\ i = j \\ 0 \mathit{if}\ i \neq j \end{cases} \qquad \psi_i(\eta_j) = \begin{cases} 1 \mathit{if}\ i = j \\ 0 \mathit{if}\ i \neq j \end{cases}$$

Legendre quadrature is used for numerical integration.

2.6. Hermite Cubic Family of Finite Elements

There are two kinds hermite cubic type finite element elements. The one in which the inter-element continuity of $\omega_0, \theta_x \equiv \partial\omega_0/\partial x \, and \, \theta_y \equiv \partial\omega_0/\partial y$ are satisfied is a conforming element. Non conforming element is one in which the continuity of normal slope is not satisfied.

2.6.1 Non Conforming Rectangular Element

The element was developed by Melosh [21] and Zienkiewicz and Cheung [22].The element has $\omega_0, \theta_x and \theta_y$ as the nodal variables as shown in Fig. 2.2. So the non-conforming element has three degrees of freedom per node. The number of nodal degrees of freedom per element is 16. The interpolation functions for this element can be written as

$$\varphi_i^e = g_{i1}(i = 1,4,7,10), \quad \varphi_i^e = g_{i2}(i = 2,5,8,11)$$

$$\varphi_i^e = g_{i3}(i = 3,6,9,12)$$

$$g_{i1} = \frac{1}{8}(1+\xi_0)(1+\eta_0)(2+\xi_0+\eta_0-\xi^2-\eta^2) \tag{2.51}$$

$$g_{i2} = \frac{1}{8}\xi_i(\xi_0-1)(1+\eta_0)(1+\xi_0)^2$$

$$g_{i3} = \frac{1}{8}\eta_i(\eta_0-1)(1+\xi_0)(1+\eta_0)^2$$

$$\xi = (x-x_c)/a, \quad \eta = (y-y_c)/b, \quad \xi_0 = \xi\xi_i, \quad \eta_0 = \eta\eta_i$$

Where (x_c, y_c) are the global coordinates of the centre of the rectangle whose sides are $2a$ and $2b$. (ξ_i, η_i) are the coordinates of the nodes in (ξ, η) coordinate system.

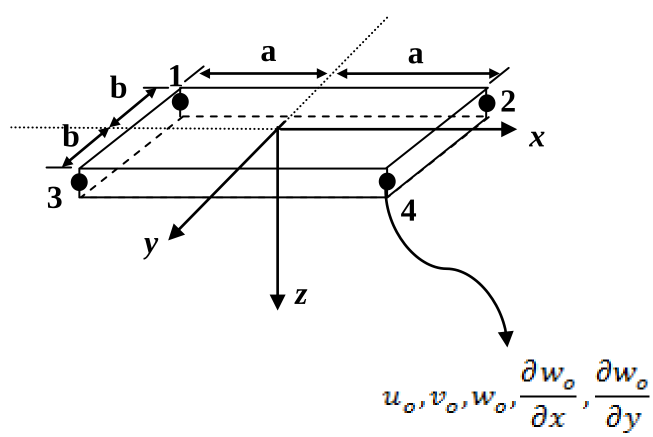

Fig.2.2. A Non conforming rectangular element

2.6.2. Conforming Rectangular Element

The element was developed by Bogner et al. [23] .The element has $\omega_0, \theta_x, \theta_y and \theta_{xy}$ as the nodal variables as shown in Fig. 2.3. The non conforming element has four degrees of freedom per node. The number of nodal degrees of freedom per element is 16. The interpolation functions for this element can be written as

$$\varphi_i^e = g_{i1}(i = 1,5,9,13), \quad \varphi_i^e = g_{i2}(i = 2,6,10,14)$$

$$\varphi_i^e = g_{i3}(i = 3,7,11,15), \qquad \varphi_i^e = g_{i4}(i = 4,8,12,16)$$

$$g_{i1} = \frac{1}{16}(\xi + \xi_i)^2(\xi_0 - 2)(\eta + \eta_i)^2(\eta_0 - 2)$$

$$g_{i2} = \frac{1}{16}\xi_i(\xi + \xi_i)^2(1 - \xi_0)(\eta + \eta_i)^2(\eta_0 - 2) \tag{2.52}$$

$$g_{i3} = \frac{1}{16}\eta_i(\xi + \xi_i)^2(\xi_0 - 2)(\eta + \eta_i)^2(1 - \eta_0)$$

$$g_{i4} = \frac{1}{16}\xi_i\eta_i(\xi + \xi_i)^2(1 - \xi_0)(\eta + \eta_i)^2(1 - \eta_0)$$

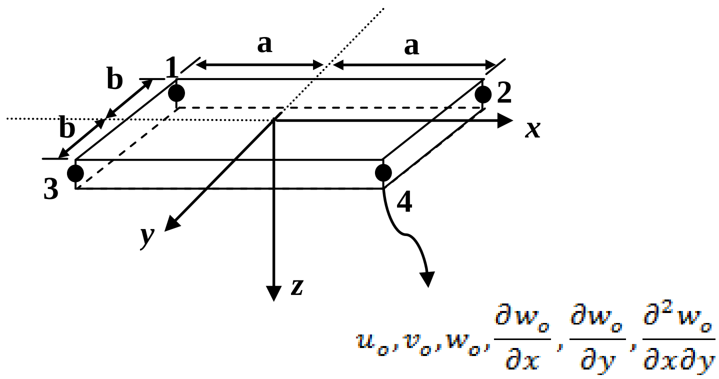

Fig.2.3**.** A Conforming rectangular element

2.7. Numerical Results

In this section numerical results obtained for all the three models are presented.

Two numerical examples were used to verify the formulations**.** Direct solver was used**.**

2.7.1 Numerical Example 1

Poisson equation over a unit square domain is

$$-\nabla^2 u = f \ in \ \Omega$$

where u is subjected to the boundary condition u=0 on all edges except on edge y=1 as shown in Fig. 2.4.

On y=1, $u(x, y)$ is specified to be

$$u(x, y) = \sin \pi x$$

The exact solution to this problem for $f = 0$ is

$$u_0(x, y) = \frac{\sin \pi x \sinh \pi y}{\sinh \pi}$$

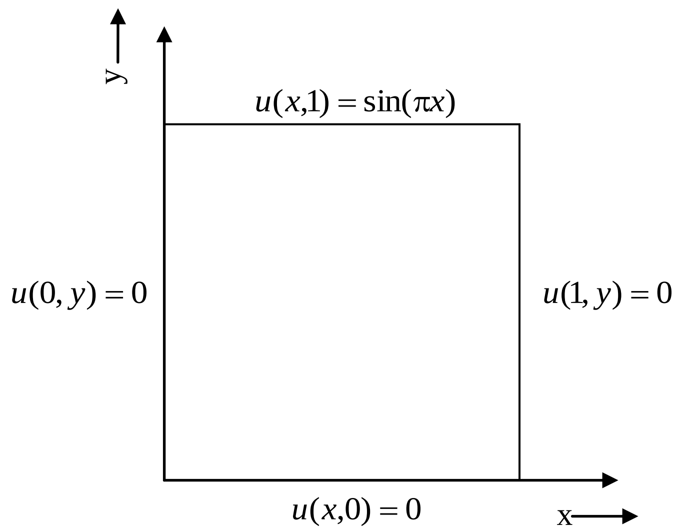

Fig. 2.4. Domain of the Poisson equation for problem in Example 1

The numerical results in case of different models are presented. The values of the field variables were compared to the actual solutions. The effect of *h*- refinement and *p*-refinement on all the models was addressed.

2.7.1.1. Numerical Results for Model 1

A 2x2 mesh with *p*-refinement was used. The results for u were plotted at y=0 and compared with the exact solution.

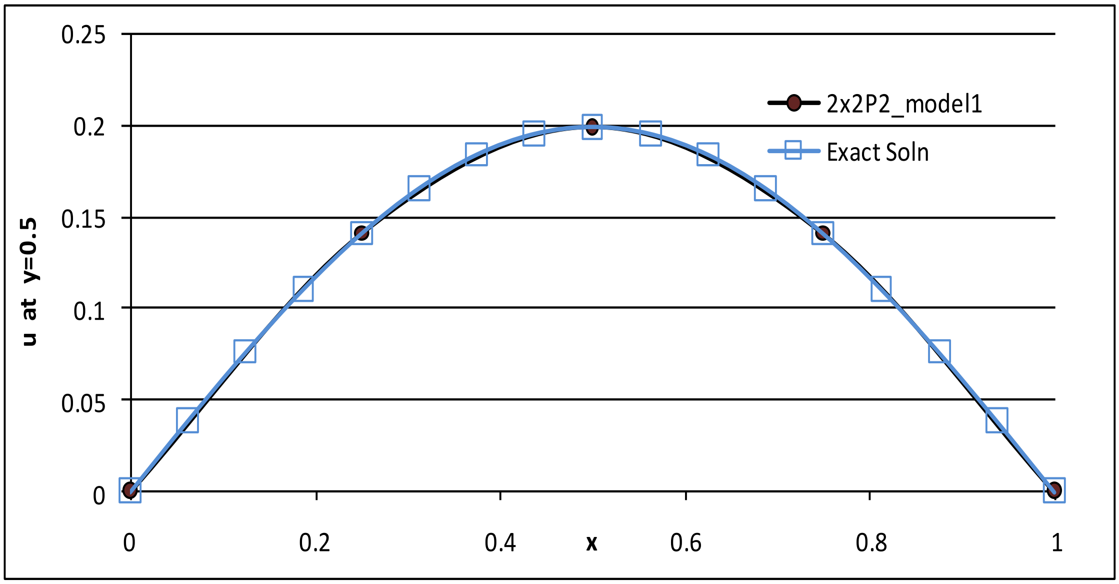

Fig.2.5. Comparison of model1solution with exact solution for 2x2 mesh, p=2

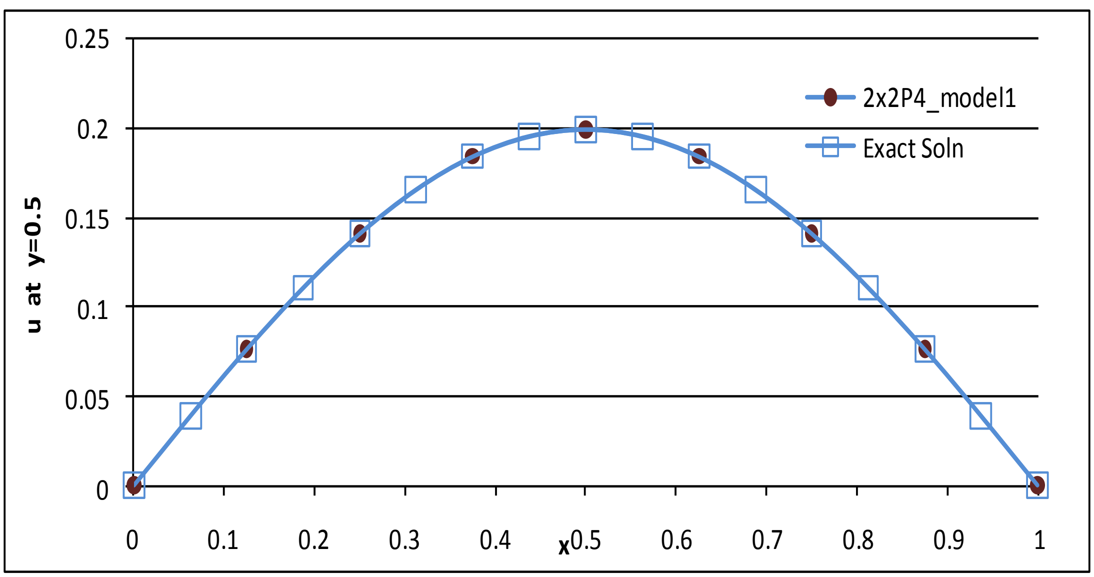

Fig.2.6. Comparison of model1solution with exact solution for 2x2 mesh, p=4

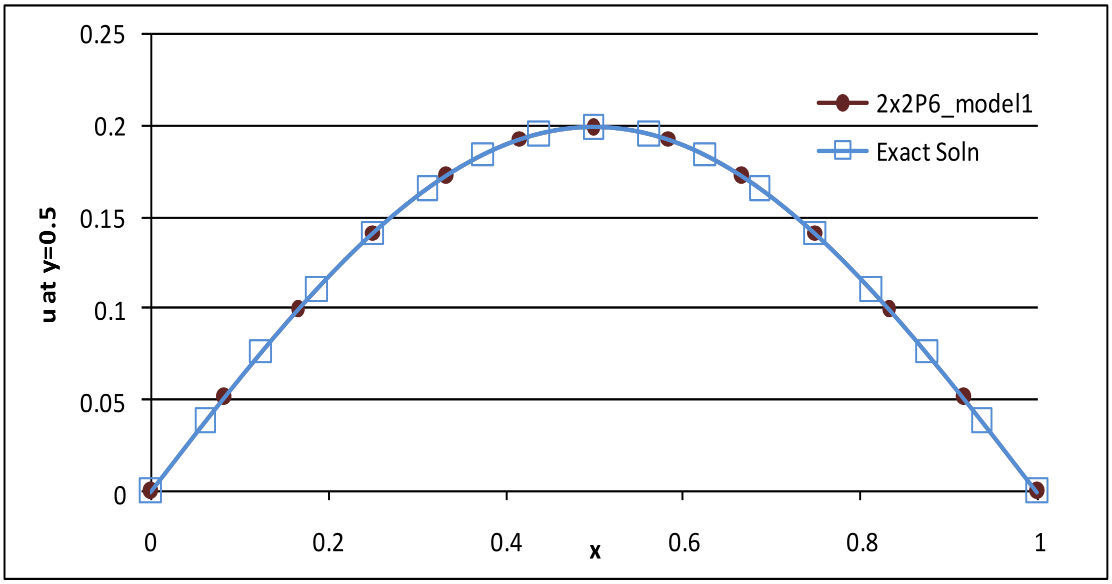

Fig.2.7. Comparison of model1solution with exact solution for 2x2 mesh, p=6

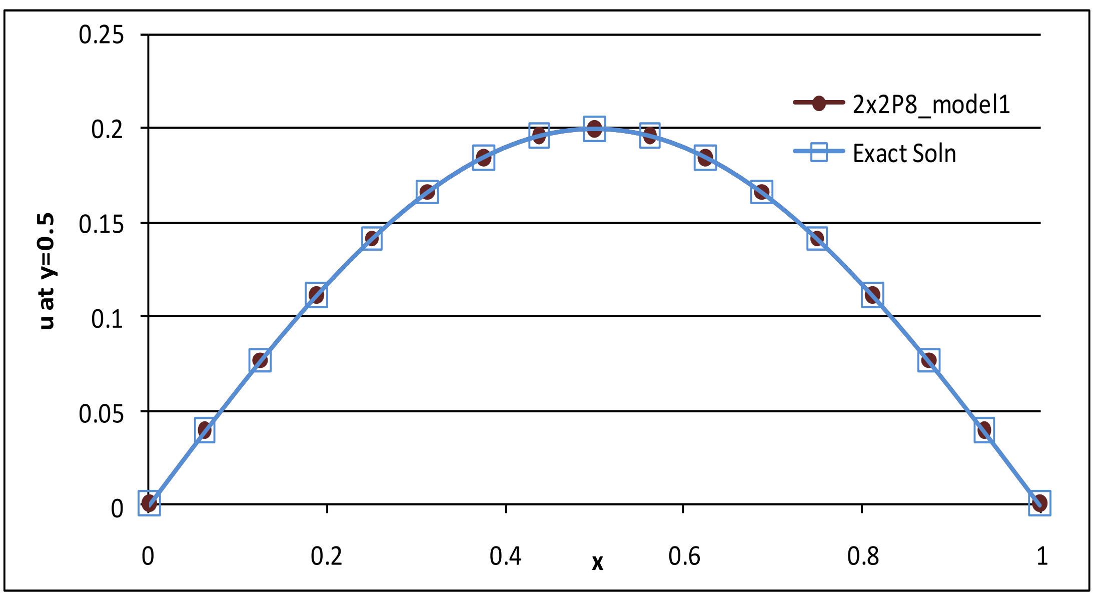

Fig.2.8. Comparison of model1solution with exact solution for 2x2 mesh, p=8

As we increase p, we see an excellent agreement between the exact solution and the results obtained from model1. Velocity fluxes have to be post-computed.

2.7.1.2. Numerical Results for Model 2

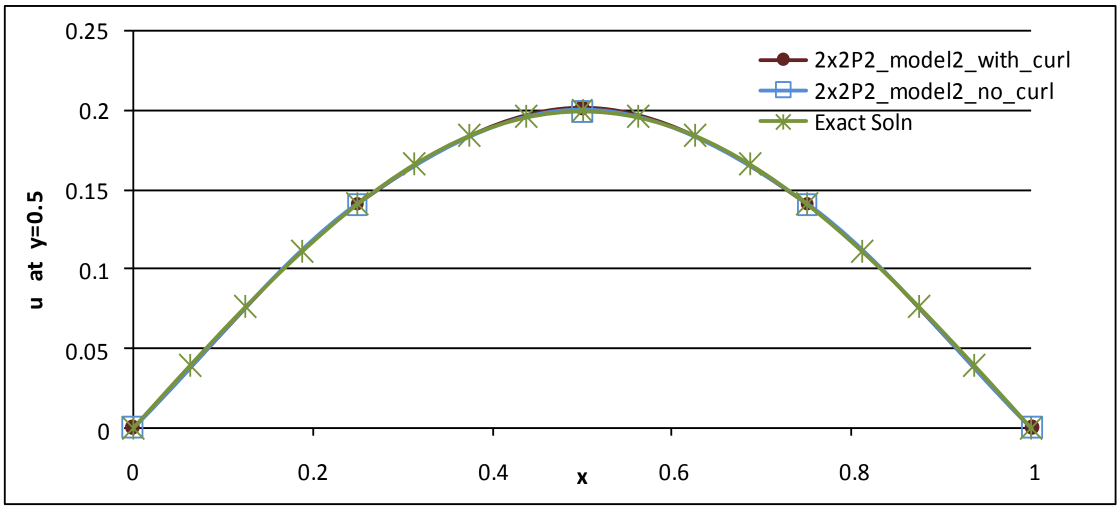

Fig.2.9. Comparison of mixed LSFEM solution with exact solution for 2x2 mesh, p=2

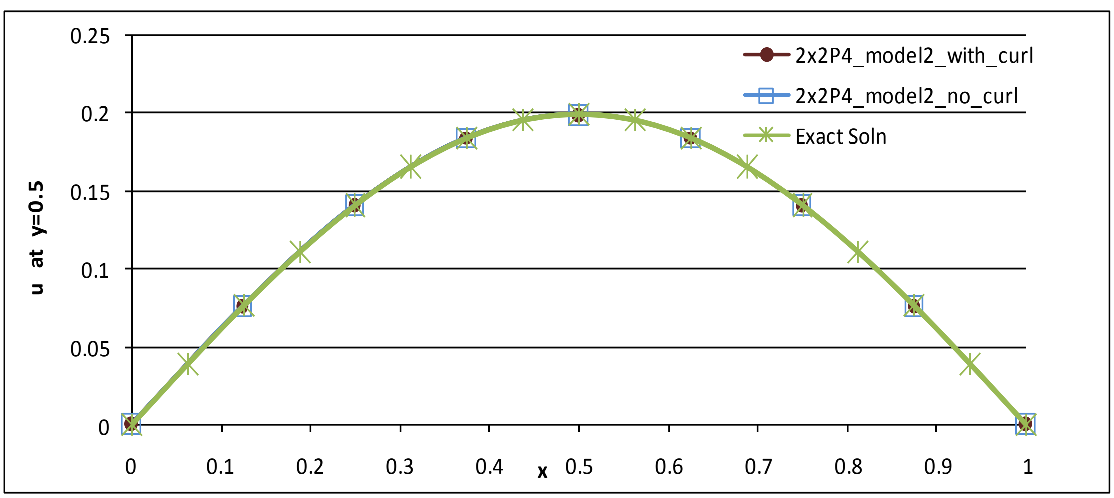

Fig.2.10. Comparison of mixed LSFEM solution with exact solution for 2x2 mesh, p=4

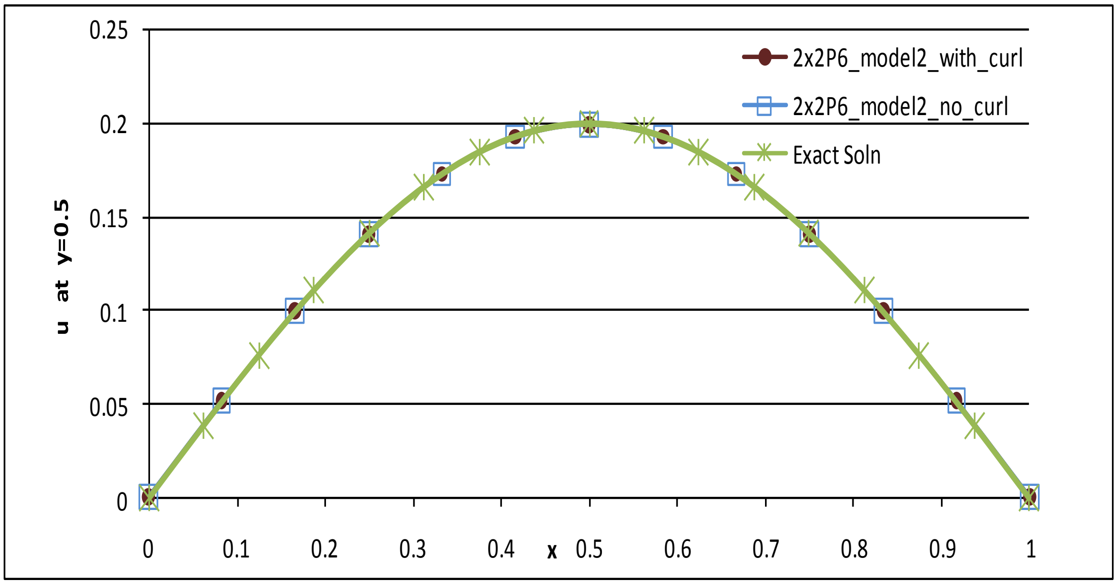

Fig.2.11. Comparison of mixed LSFEM solution with exact solution for 2x2 mesh, p=6

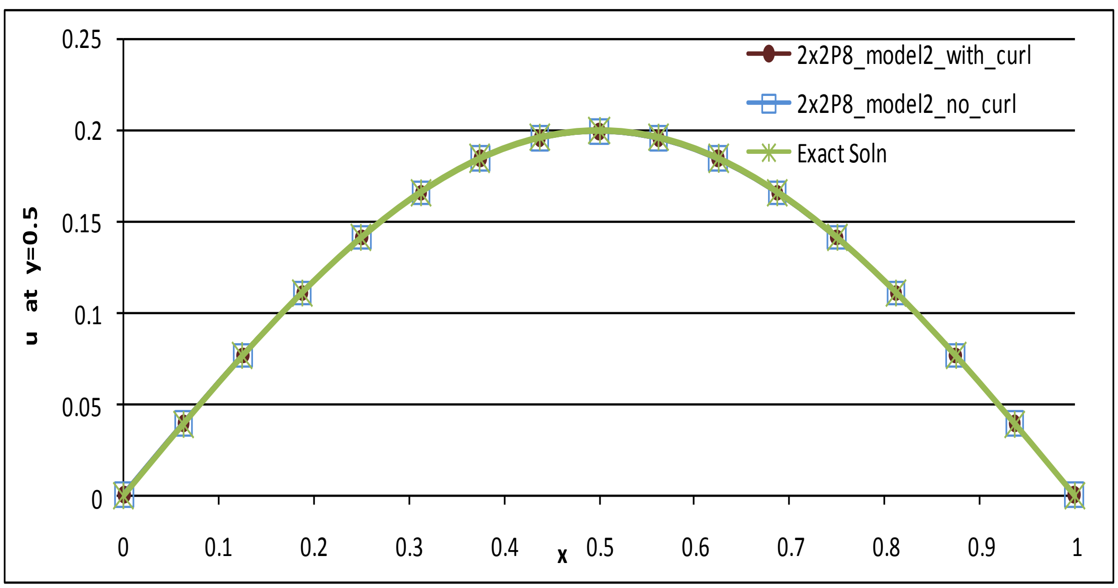

Fig.2.12. Comparison of mixed LSFEM solution with exact solution for 2x2 mesh, p=8

The solution of u along y=0.5 were plotted. Model 2 based on LSFEM shows excellent agreement with the exact solution. As p level was gradually increased the solutions do not depend on the grid size. We can have a coarse mesh of 2x2 mesh. The results obtained with and without the curl constraint (added to insure coersivity) were almost the same. The fluxes are primary variables and hence postcomputation is not needed.

2.7.1.3. Numerical Results for Model 3

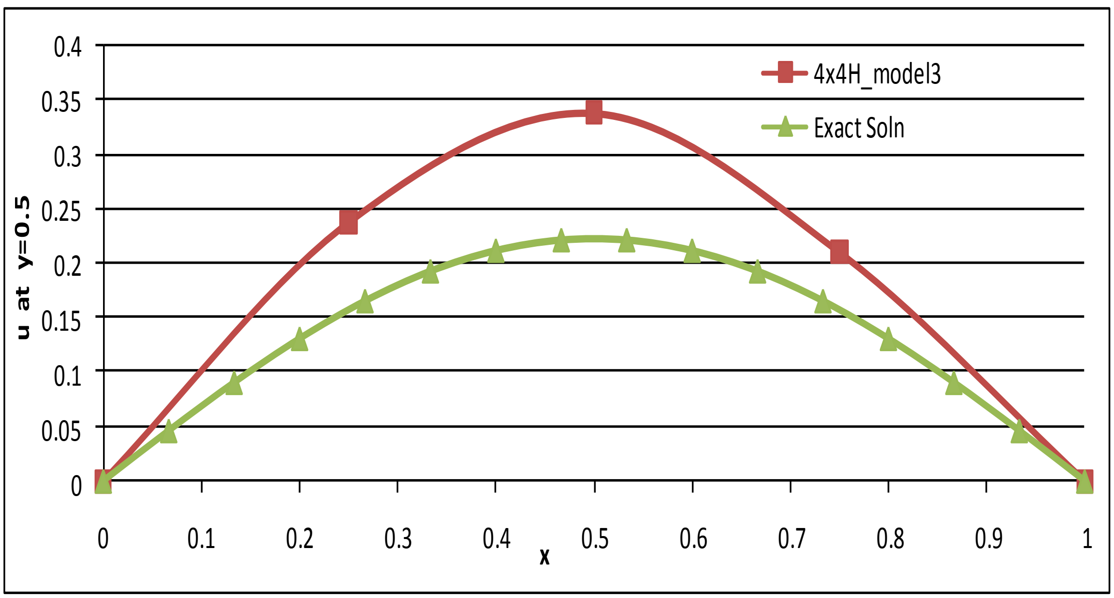

Fig.2.13. Comparison of LSFEM solution with exact solution for 4x4 mesh

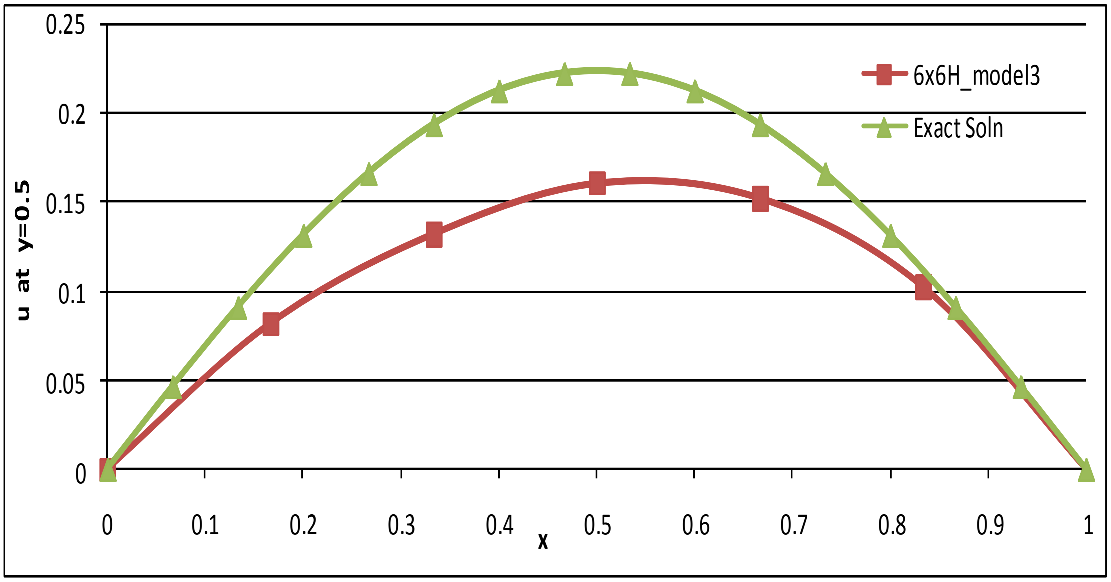

Fig. 2.14. Comparison of LSFEM solution with exact solution for 6x6 mesh

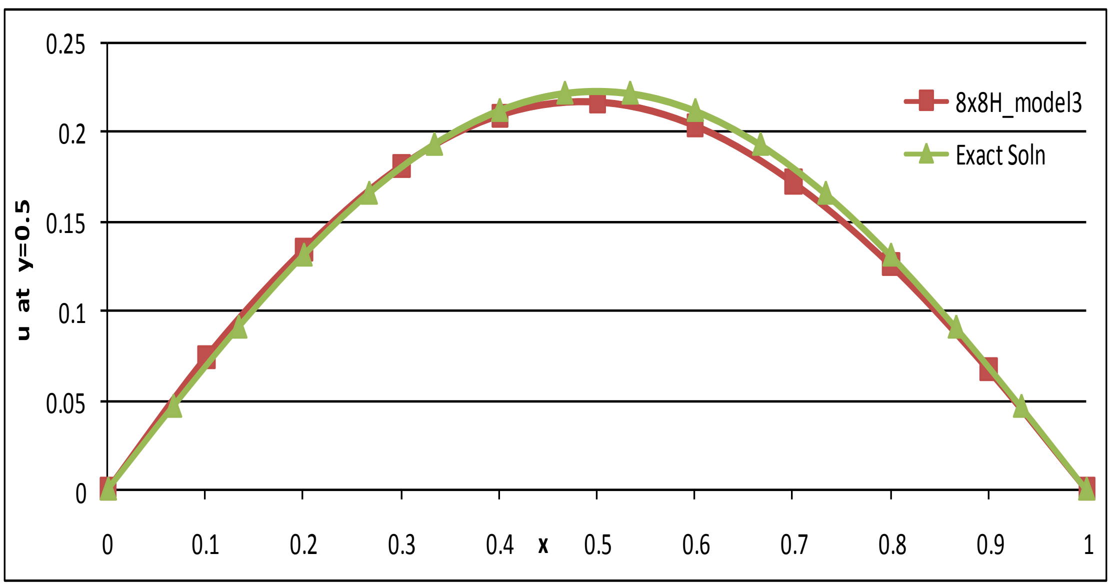

Fig. 2.15. Comparison of LSFEM solution with exact solution for 8x8 mesh

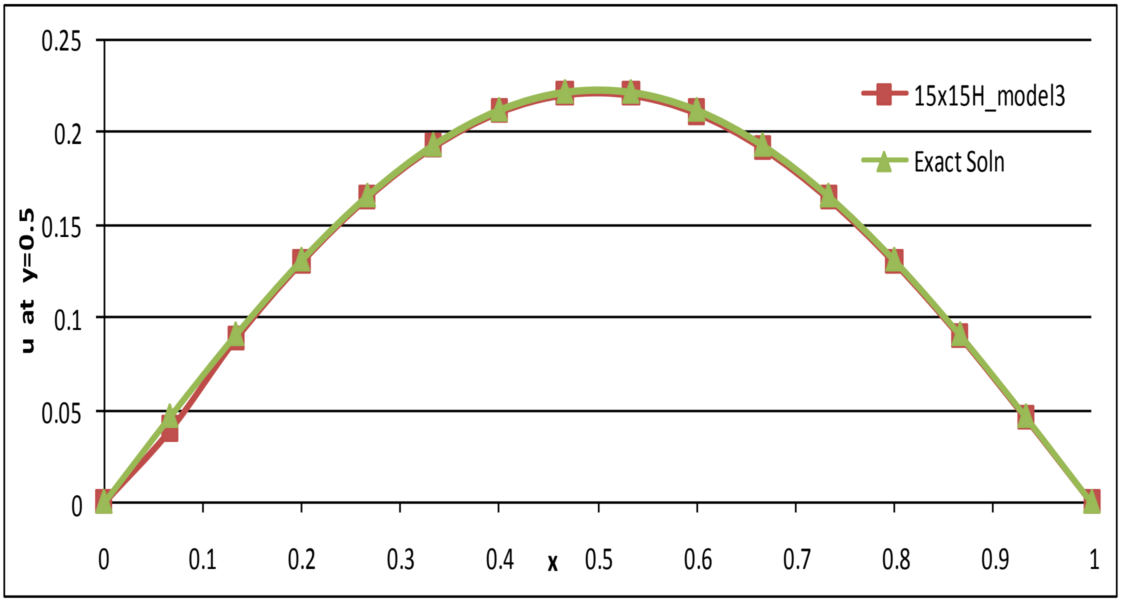

Fig.2.16. Comparison of LSFEM solution with exact solution for 15x15 mesh

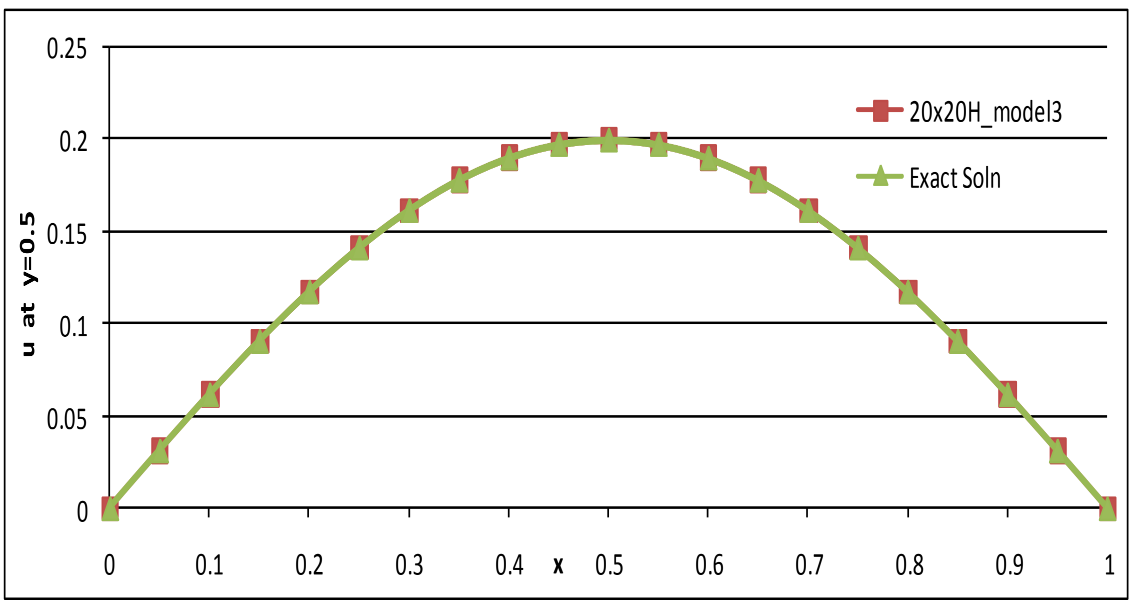

Fig.2.17. Comparison of LSFEM solution with exact solution for 20x20 mesh

For model 3 we use a conforming rectangular element. The mesh was refined from a 4x4 mesh to a 20x20 mesh. Results were plotted for u at y=0.5. With *h* refinement the results show agreement with the exact solution. However the numerical results for fluxes were not close to the exact solution even with a 20x20 mesh.

2.7.2. Numerical Example 2

Poisson equation over a unit square domain is

$$-\nabla u = f \ , \ \text{in } \Omega$$

where, the boundary are shown in Fig.2.17.

The series solution to this problem for $f = 1$ is

$$u_0(x, y) = \frac{1}{2}\left[(1 - y^2) + 4\sum_{n=1}^{\infty} \frac{(-1)^n \cos\alpha_n y \cosh\alpha_n x}{\alpha_n{}^3 \cosh\alpha_n}\right], \alpha_n = (2n-1)\pi/2$$

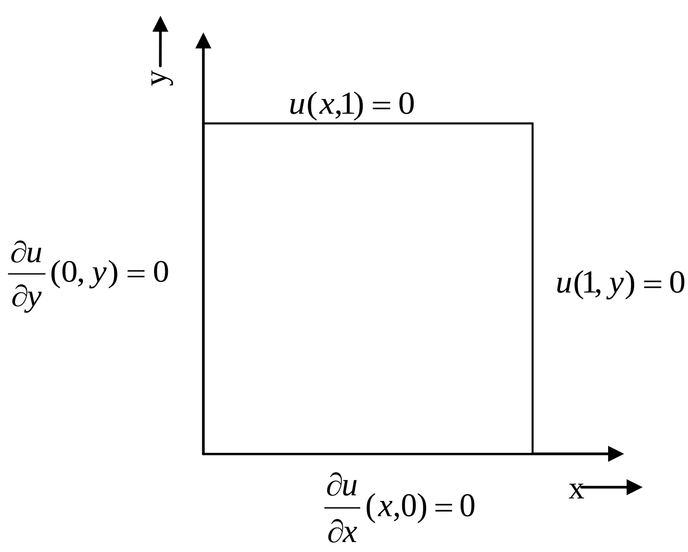

Fig.2.18.Domain of the Poisson equation for problem in Example 2

The results obtained for u (x,0) was compared with the series solution. The domain was descretized using a 2x2 mesh.

2.7.2.1 Numerical Results for Model 1

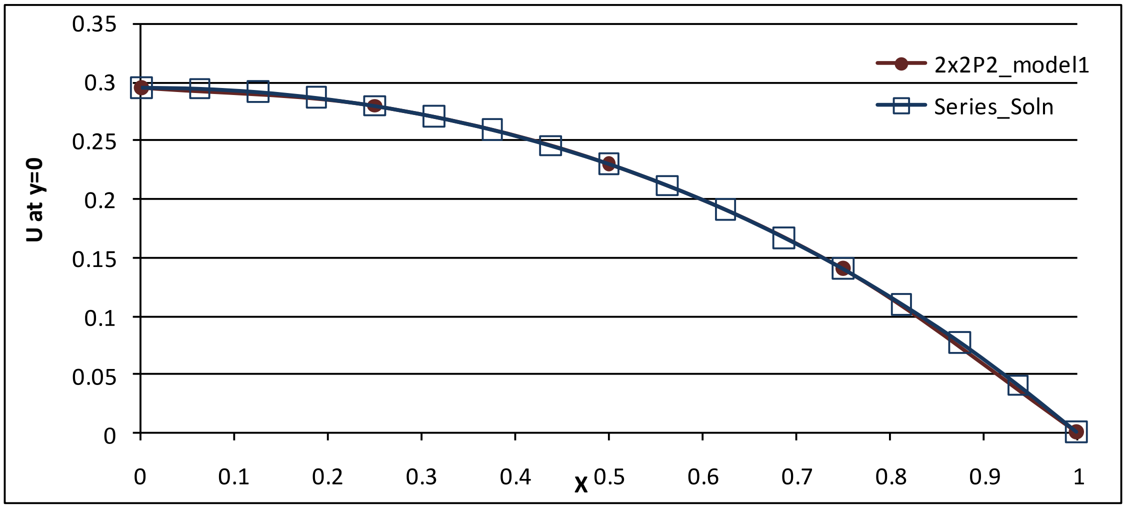

Fig.2.19.Comparison of model1 solution with series solution for 2x2 mesh, p=2

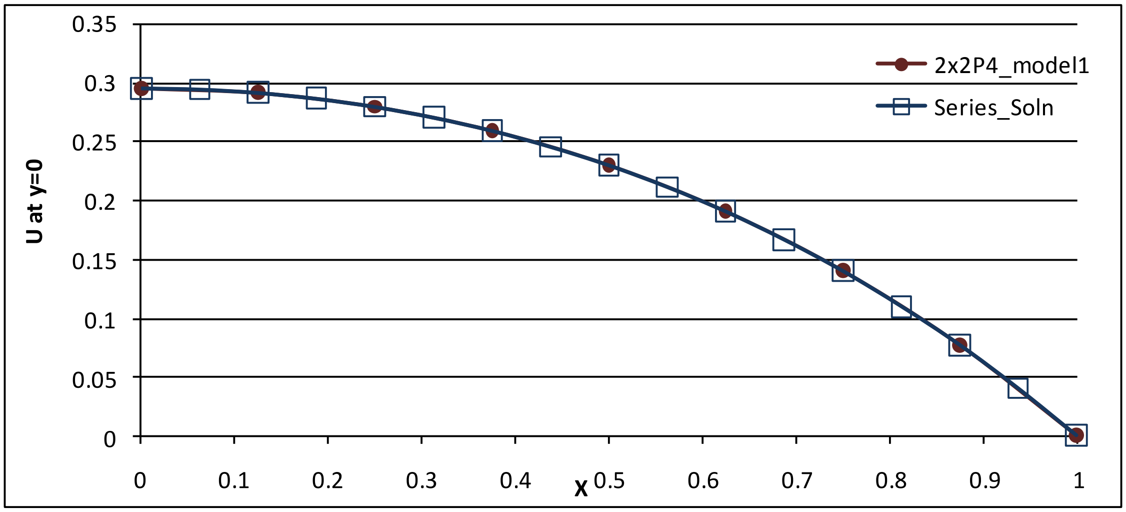

Fig.2.20.Comparison of model1 solution with series solution for 2x2 mesh, p=4

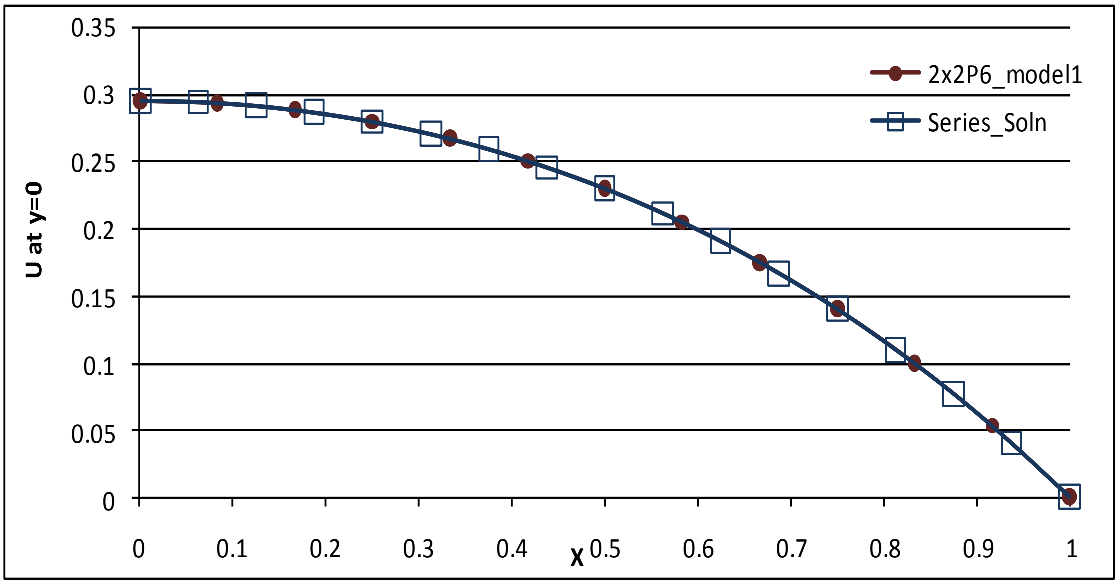

Fig.2.21.Comparison of model1 solution with series solution for 2x2 mesh, p=6

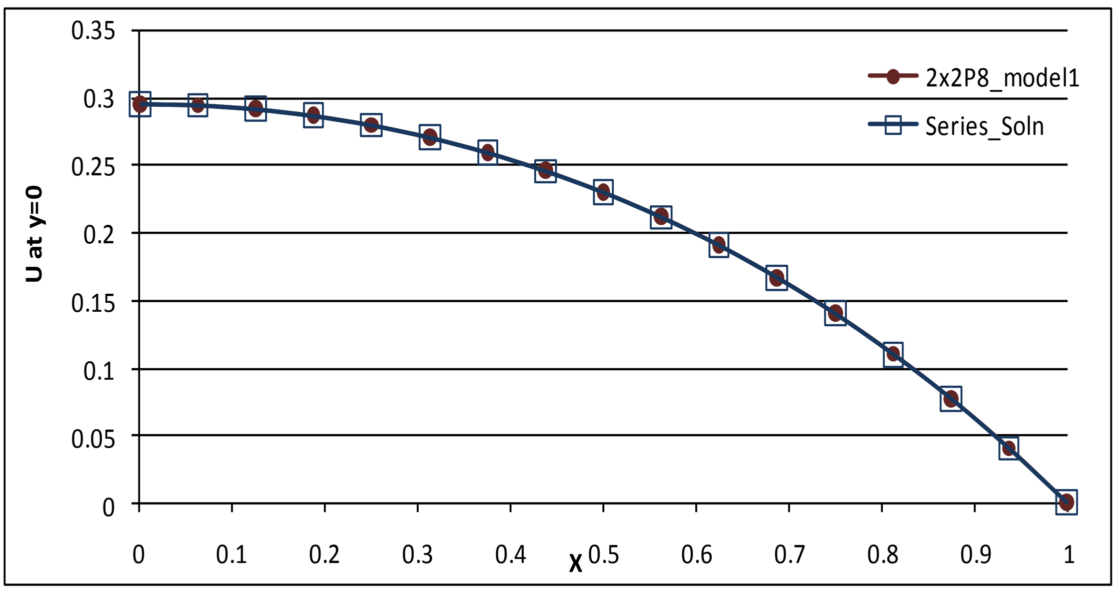

Fig.2.22.Comparison of model1 solution with series solution for 2x2 mesh, p=8

For example 2, results for u (x,0) were plotted and compared with the series solution. With model1 accurate results were obtained using 2x2 mesh with second order polynomial approximation.

2.7.2.2. Numerical Result for Model 2

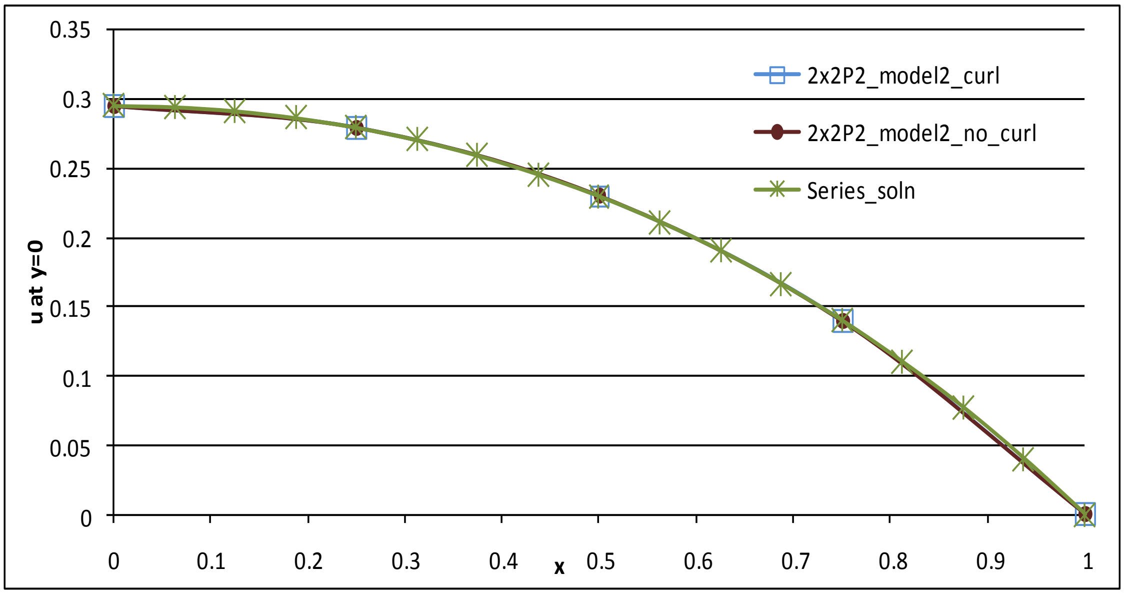

Fig.2.23. Comparison of mixed LSFEM solution with series solution for 2x2 mesh, p=2

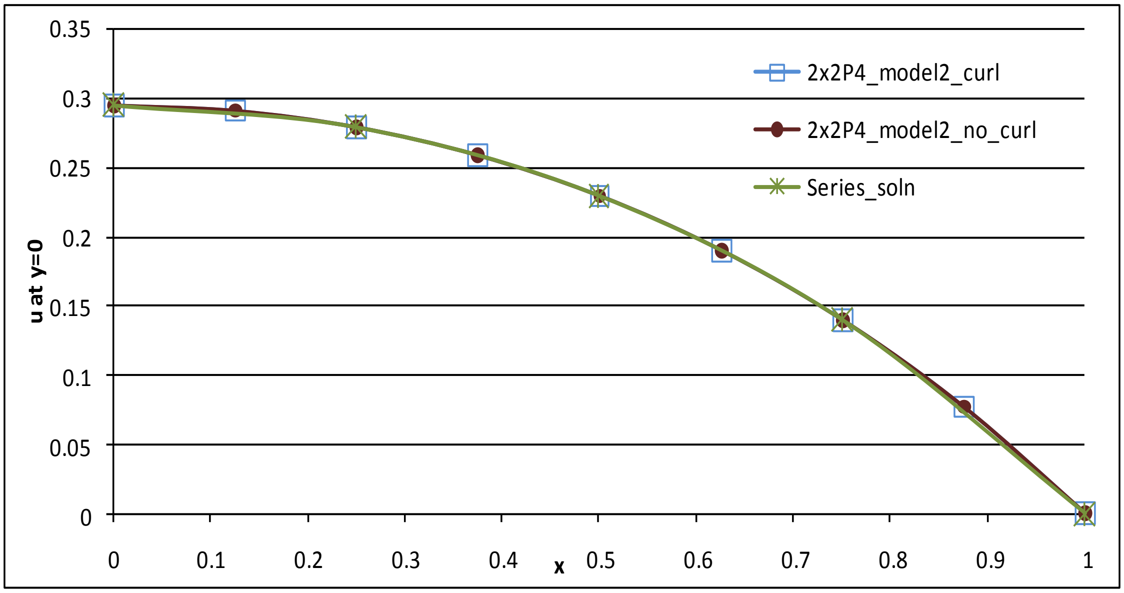

Fig.2.24. Comparison of mixed LSFEM solution with series solution for 2x2 mesh, p=4

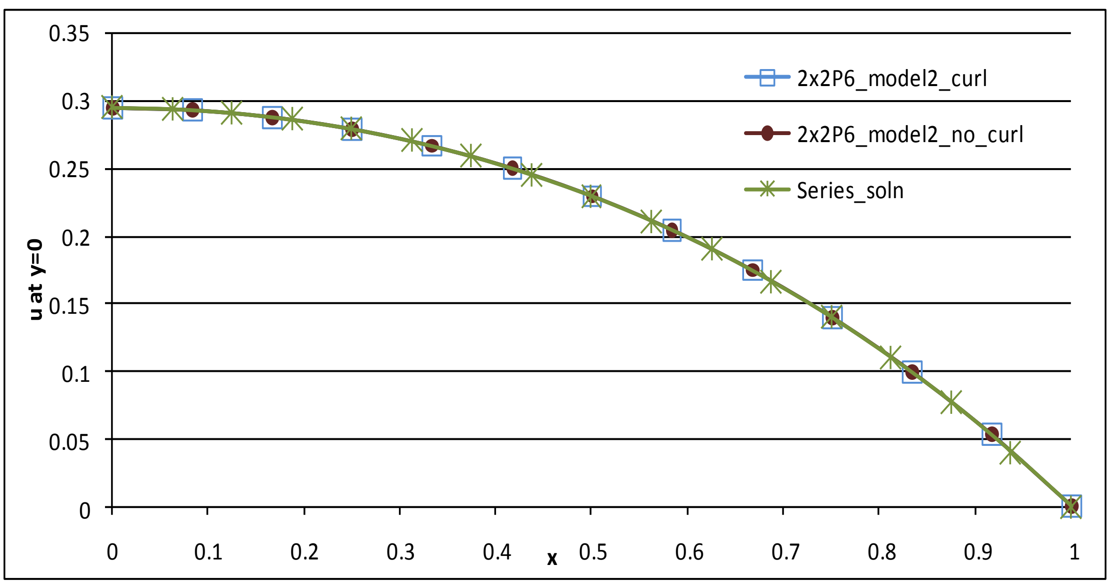

Fig.2.25. Comparison of mixed LSFEM solution with series solution for 2x2 mesh, p=6

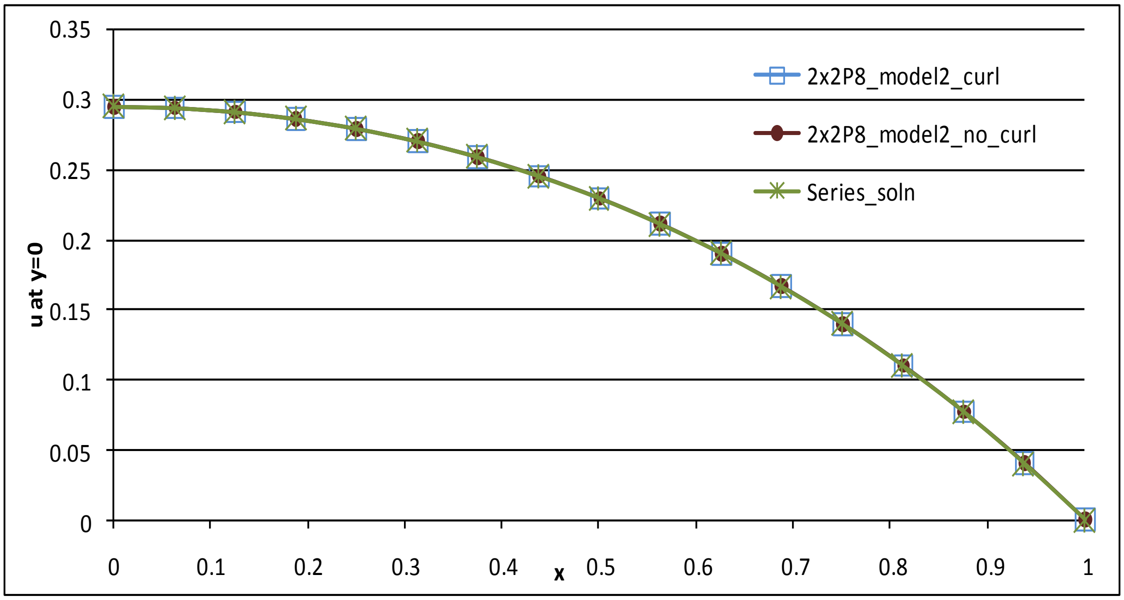

Fig.2.26. Comparison of mixed LSFEM solution with series solution for 2x2 mesh, p=8

CHAPTER III

FINITE ELEMENT MODELS FOR

NAVIER-STOKES EQUATION

3.1. Incompressible Navier-Stokes Equations

Claude-Louis Navier and George S. Stokes developed the exact equations that govern the flow of Newtonian fluids. On appropriately generalizing these equations for compressible flow, we get the Navier-Stokes equations. They are one of the most useful sets of equations because they describe the physics of a large number of phenomena of academic and economic interest.

In this chapter governing equations of incompressible fluid flow will be reviewed, develop finite element models based on various formulations, and describe the flow chart for implementing these models into computer programs.

3.1.1 Governing Equations

Motion of a general fluid is governed by several equations. The basic relations are the laws of conservation of mass (continuity relation), momentum and energy. Then there are constitutive relations for surface stresses and heat flux. These are a set of non-linear partial differential equation in terms of velocity vector, pressure and temperature. When temperature effect is negligible, we can decouple Navier-Stokes equation and energy equation. For isothermal flows, we solve the continuity equation and the conservation of linear momentum equations. The governing equations presented here are based on the Eulerian description.

3.1.1.1 Conservation of Mass

The principle of conservation of mass can be stated as the time rate of change of mass in a control volume is equal to the rate of inflow of mass through the control surface. In other words, the time rate of change of the mass of a material region is zero and this is called the continuity equation.

$$\frac{\partial \rho}{\partial t} + \nabla.(\rho \mathbf{v}) = 0 \tag{3.1}$$

where, ρ is the density (kg / m^3) of the medium, **v** is the velocity vector (m/s), and **∇** is the vector differential operator. Introducing the material derivative (D/Dt)

$$\frac{D}{Dt} = \frac{\partial}{\partial t} + \mathbf{v}.\nabla \tag{3.2}$$

For steady-state conditions, the continuity equation becomes

$$\nabla.(\rho \mathbf{v}) = 0 \tag{3.3}$$

When the density changes following a fluid particle are negligible we have $D\rho/Dt=0$. For incompressible flow continuity equation (3.3) simplifies to

$$\nabla.\mathbf{v} = 0 \tag{3.4}$$

Equation (3.4) can be described as the rate of increase of the volume of a material particle. Since the velocity field **v** is required to satisfy the equations of motion derived in the next section, equation (3.4) is known as a constraint among the velocity components.

3.1.1.2 Conservation of Linear Momentum

The principle of conservation of linear momentum (or Newton's Second Law of motion) states that the time rate of change of linear momentum of a given set of particles is equal to the vector sum of all external forces acting on the particles of the set, provided Newton's Third Law of action and reaction governs the internal forces. Newton's Second Law can be written as

$$\rho \frac{D\mathbf{v}}{Dt} = \nabla . \boldsymbol{\sigma} + \rho \mathbf{f} \qquad (3.5)$$

where, $\boldsymbol{\sigma}$ is the Cauchy stress tensor (N/m^2) and **f** is the body force vector, measured per unit mass. Equation (3.5) is known as the Navier-Stokes equations.

3.1.1.3 Conservation of Angular Momentum

The principle of conservation of angular momentum can be stated as the time rate of change of the total moment of momentum of a given set of particles is equal to the vector sum of the moments of the external forces acting on the system. In the absence of distributed couples, the principle leads to the symmetry of the stress tensor:

$$\boldsymbol{\sigma} = (\boldsymbol{\sigma})^T \qquad (3.6)$$

3.1.1.4. Constitutive Equations

If we consider the fluid to be viscous and incompressible, the total stress σ is given by

$$\boldsymbol{\sigma} = \boldsymbol{\tau} + (-P)\mathbf{I} \tag{3.7}$$

where, P is the hydrostatic pressure, **I** is the unit tensor, and $\boldsymbol{\tau}$ is the viscous stress tensor.

For Newtonian isotropic fluid $\boldsymbol{\tau}$ is written as

$$\boldsymbol{\tau} = \lambda(tr[\mathbf{D}])\mathbf{I} + 2\mu\mathbf{D} \tag{3.8}$$

where D is the strain rate tensor, defined by,

$$\mathbf{D} = \frac{1}{2}\left[(\nabla\mathbf{v}) + (\nabla\mathbf{v})^T\right] \tag{3.9}$$

λ ,μ are the Lame constant. For an incompressible fluid $tr[\mathbf{D}]$=0 so equation (3.8) becomes

$$\boldsymbol{\tau} = 2\mu\mathbf{D} \tag{3.10}$$

Let Ω denote the open bounded domain in $\Re^n, n = 2 or 3$ and Γ denote the sufficiently smooth boundary of Ω .

The equations can be expressed in terms of velocity components and pressure*(u* ,v ,*P)* for Newtonian, isotropic, viscous, incompressible fluid flow in two-dimension. Where u, v are the velocity in x and y direction respectively.

$$\frac{\partial u}{\partial x} + \frac{\partial v}{\partial y} = 0 \tag{3.11}$$

$$\rho\left(\frac{\partial u}{\partial t} + u\frac{\partial u}{\partial x} + v\frac{\partial u}{\partial y}\right) + \frac{\partial P}{\partial x} - \frac{\partial}{\partial x}\left(2\mu\frac{\partial u}{\partial x}\right) - \frac{\partial}{\partial y}\left(\mu\left(\frac{\partial u}{\partial y} + \frac{\partial v}{\partial x}\right)\right) - \rho f_x = 0 \tag{3.12}$$

$$\rho\left(\frac{\partial v}{\partial t}+u\frac{\partial v}{\partial x}+v\frac{\partial v}{\partial y}\right)+\frac{\partial P}{\partial y}-\frac{\partial}{\partial y}\left(2\mu\frac{\partial v}{\partial y}\right)-\frac{\partial}{\partial x}\left(\mu\left(\frac{\partial u}{\partial y}+\frac{\partial v}{\partial x}\right)\right)-\rho f_y=0$$

The above equations are known as Navier-Stokes equations in two dimensions and reduce to Stokes flow for steady, slow and viscous flows.

$$\frac{\partial u}{\partial x}+\frac{\partial v}{\partial y}=0$$

$$\frac{\partial P}{\partial x}-\frac{\partial}{\partial x}\left(2\mu\frac{\partial u}{\partial x}\right)-\frac{\partial}{\partial y}\left(\mu\left(\frac{\partial u}{\partial y}+\frac{\partial v}{\partial x}\right)\right)-\rho f_x=0 \tag{3.13}$$

$$\frac{\partial P}{\partial y}-\frac{\partial}{\partial y}\left(2\mu\frac{\partial v}{\partial y}\right)-\frac{\partial}{\partial x}\left(\mu\left(\frac{\partial u}{\partial y}+\frac{\partial v}{\partial x}\right)\right)-\rho f_y=0$$

For stokes flow there are no nonlinear terms as the convective terms are zero.

3.2. Conventional Mixed Model

To get the weak form, we need the weighted integral statement of equations (3.13).

The weighted-integral statements over a typical element Ω^e are given by

$$\int_{\Omega^e} w_1\left(\frac{\partial u}{\partial x}+\frac{\partial v}{\partial y}\right)dxdy=0 \tag{3.14}$$

$$\int_{\Omega^e} w_2\left\{\rho\left(u\frac{\partial u}{\partial x}+v\frac{\partial u}{\partial y}\right)+\frac{\partial P}{\partial x}-\frac{\partial}{\partial x}\left(2\mu\frac{\partial u}{\partial x}\right)-\frac{\partial}{\partial y}\left(\mu\left(\frac{\partial u}{\partial y}+\frac{\partial v}{\partial x}\right)\right)-\rho f_x\right\}dxdy=0 \tag{3.15}$$

$$\int_{\Omega^e} w_3\left\{\rho\left(u\frac{\partial v}{\partial x}+v\frac{\partial v}{\partial y}\right)+\frac{\partial P}{\partial y}-\frac{\partial}{\partial y}\left(2\mu\frac{\partial v}{\partial y}\right)-\frac{\partial}{\partial x}\left(\mu\left(\frac{\partial u}{\partial y}+\frac{\partial v}{\partial x}\right)\right)-\rho f_y\right\}dxdy=0 \tag{3.16}$$

where, (w_1, w_2, w_3) are the weight functions.

Integrating by parts , we get the weak forms.

$$\int_{\Omega^e} w_1 \left(\frac{\partial u}{\partial x} + \frac{\partial v}{\partial y} \right) dxdy = 0 \tag{3.17}$$

$$\int_{\Omega^e} \left\{ w_2 \rho \left(u \frac{\partial u}{\partial x} + v \frac{\partial u}{\partial y} \right) + w_2 \frac{\partial P}{\partial x} + \frac{\partial w_2}{\partial x} \left(2\mu \frac{\partial u}{\partial x} \right) + \frac{\partial w_2}{\partial y} \left(\mu \left(\frac{\partial u}{\partial y} + \frac{\partial v}{\partial x} \right) \right) - w_2 \rho f_x \right\} dxdy - \oint_{\Gamma^e} w_2 t_x ds = 0 \tag{3.18}$$

$$\int_{\Omega^e} \left\{ w_3 \rho \left(u \frac{\partial v}{\partial x} + v \frac{\partial v}{\partial y} \right) + w_3 \frac{\partial P}{\partial y} + \frac{\partial w_3}{\partial y} \left(2\mu \frac{\partial v}{\partial y} \right) + \frac{\partial w_3}{\partial x} \left(\mu \left(\frac{\partial u}{\partial y} + \frac{\partial v}{\partial x} \right) \right) - w_3 \rho f_y \right\} dxdy - \oint_{\Gamma^e} w_3 t_y ds = 0 \tag{3.19}$$

where, (t_x, t_y) are the boundary traction components.

$$t_x = \left(2\mu \frac{\partial u}{\partial x} - P \right) n_x + \mu \left(\frac{\partial u}{\partial y} + \frac{\partial v}{\partial x} \right) n_y \tag{3.21}$$

$$t_y = \left(2\mu \frac{\partial v}{\partial y} - P \right) n_y + \mu \left(\frac{\partial u}{\partial y} + \frac{\partial v}{\partial x} \right) n_x \tag{3.22}$$

The field variables are approximated by

$$u^h(x,y) = \sum_{i=1}^{N} \psi_i(x,y) u^i, \qquad v^h(x,y) = \sum_{i=1}^{N} \psi_i(x,y) v^i \tag{3.23}$$

$$P^h(x,y) = \sum_{i=1}^{N} \phi_i(x,y) P^i,$$

where, ψ, ϕ are the Lagrange family of interpolation function and u^i, v^i, P^i are the nodal values of u^h, v^h, P^h. The weak form contains first derivatives of velocities and no derivatives on P, so the interpolation function used for P is one order less than that used for velocities. On substituting these approximations, the finite element model is obtained.

3.3. Reduced Integration Penalty Model

The penalty finite element model is obtained by substituting *p* by the equation

$$p = -\gamma(\nabla.\mathbf{v}) \tag{3.24}$$

where, γ is the penalty parameter. The continuity equation is used like a constraint. Pressure variable is removed from the system of equations. The disadvantage of this method is that a very high penalty parameter $10^8 - 10^{12}$ is required to obtain accurate results. When the value of γ is very large, the viscous terms become negligibly small compared to the penalty terms in a computer. This results in a trivial solution. This condition is termed as ‘locking’. To avoid locking, the penalty terms have to be underintegrated [24]. However, as we do *p*-refinement, the resulting equations become less sensitive to locking.

3.4. Least-Squares Finite Element Model (Velocity Gradient Based)

Here we present the mixed least-squares finite element model of the Navier-Stokes equations. After substituting the approximations for the field variables, we get the residuals and least-squares method has the property of minimizing these residuals. Least-squares method provides a variational framework for Navier-Stokes equations. Main ideas of least-squares method are described using the steady Stokes flow problem.

Considering steady, viscous, incompressible Stokes flow problem, the governing differential equations are:

$$-\mu\nabla.\left[(\nabla\mathbf{v})+(\nabla\mathbf{v})^T\right]+\nabla P-\rho\mathbf{f}=0 \tag{3.25}$$

$$\nabla.\mathbf{v}=0 \tag{3.26}$$

where, $\mathbf{v}$ is the velocity vector, with v_x and v_y being the horizontal and vertical component of velocity for two-dimensional flow. P is the pressure and $\mathbf{f}$ is the body force vector. On substituting suitable finite element approximations of the field variables $(\mathbf{v},P)$ into the differential equations, the following residual equations are obtained.

$$R_1=-\mu\nabla.\left[(\nabla\mathbf{v})+(\nabla\mathbf{v})^T\right]+\nabla P-\rho\mathbf{f} \tag{3.27}$$

$$R_2=\nabla.\mathbf{v} \tag{3.28}$$

Least-squares principle requires to minimize I, where

$$I(\mathbf{v},P)\equiv\frac{1}{2}\int_{\Omega^e}(R_1^2+R_2^2)$$

$$=\frac{1}{2}\left(\left\|-\mu\nabla.\left[(\nabla\mathbf{v})+(\nabla\mathbf{v})^T\right]+\nabla P-\rho\mathbf{f}\right\|_0^2+\left\|\nabla.\mathbf{v}\right\|_0^2\right)$$

and $\|\cdot\|$ denotes the $L_2(\Omega^e)$- norm as described by equation (3.29)

$$\|u\|_0^2=\tfrac{1}{2}\int_{\Omega^e}|u|^2\,d\mathbf{x} \tag{3.29}$$

Setting $\delta I=0$ is equivalent to the variational problem where, we have to find $(\mathbf{v},P)\in S_h$ such that for all $(\mathbf{w},Q)$ in the same vector space the following equation holds

$$B((\mathbf{w},Q),(\mathbf{v},P)) = l((\mathbf{w},Q))$$

where $B(\cdot,\cdot)$ is a symmetric bilinear form and $l((\mathbf{w},Q))$ is a linear form

$$B((\mathbf{v},P),(\mathbf{w},Q)) = \int_{\Omega^e} \left\{-\mu\nabla.\left[(\nabla\mathbf{v})+(\nabla\mathbf{v})^T\right]+\nabla P\right\}\cdot\left\{-\mu\nabla.\left[(\nabla\mathbf{w})+(\nabla\mathbf{w})^T\right]+\nabla Q\right\}d\mathbf{x}$$
$$+\int_{\Omega^e}(\nabla.\mathbf{v})(\nabla.\mathbf{w})d\mathbf{x}$$
$$l((\mathbf{w},Q)) = \int_{\Omega^e}\rho\mathbf{f}\cdot\left\{-\mu\nabla\cdot\left[(\nabla\mathbf{w})+(\nabla\mathbf{w})^T\right]+\nabla Q\right\}d\mathbf{x}$$

3.4.1. Finite Element Model for Navier-Stokes

In the case of the Navier-Stokes equations, we shall consider the least-squares iterative penalty finite element model that includes the velocities and velocity gradients as the variables to solve two-dimensional flows of viscous incompressible fluids. Numerical results will be presented for the well-known wall-driven cavity flow problem.

The Navier-Stokes equation (two-dimension) in component form is written as

$$\frac{\partial\hat{u}}{\partial\hat{x}}+\frac{\partial\hat{v}}{\partial\hat{y}}=0$$

$$\hat{u}\frac{\partial\hat{u}}{\partial\hat{x}}+\hat{v}\frac{\partial\hat{u}}{\partial\hat{y}}+\frac{1}{\rho}\frac{\partial\hat{P}}{\partial\hat{x}}-\frac{1}{\rho}\frac{\partial}{\partial\hat{x}}\left(2\mu\frac{\partial\hat{u}}{\partial\hat{x}}\right)-\frac{1}{\rho}\frac{\partial}{\partial\hat{y}}\left(\mu\left(\frac{\partial\hat{u}}{\partial\hat{y}}+\frac{\partial\hat{v}}{\partial\hat{x}}\right)\right)-\rho f_x=0 \qquad (3.30)$$

$$\hat{u}\frac{\partial\hat{v}}{\partial\hat{x}}+\hat{v}\frac{\partial\hat{v}}{\partial\hat{y}}+\frac{1}{\rho}\frac{\partial\hat{P}}{\partial\hat{y}}-\frac{1}{\rho}\frac{\partial}{\partial\hat{y}}\left(2\mu\frac{\partial\hat{v}}{\partial\hat{y}}\right)-\frac{1}{\rho}\frac{\partial}{\partial\hat{x}}\left(\mu\left(\frac{\partial\hat{u}}{\partial\hat{y}}+\frac{\partial\hat{v}}{\partial\hat{x}}\right)\right)-\rho f_y=0$$

Assuming constant values for ρ, μ, f_x and f_y the following dimensionless variables can be used:

$$x=\frac{\hat{x}}{L}, \quad y=\frac{\hat{y}}{L}, \quad P=\frac{\hat{P}}{\rho U_0^2}, \quad u=\frac{\hat{u}}{U_0^2}, \quad v=\frac{\hat{v}}{U_0^2},$$

substituting these dimensionless variables in equations (3.30) we get the following nondimensionless equations:

$$\frac{\partial u}{\partial x}+\frac{\partial v}{\partial y}=0$$

$$u\frac{\partial u}{\partial x}+v\frac{\partial u}{\partial y}+\frac{\partial P}{\partial x}-\frac{\partial}{\partial x}\left(\frac{2}{\mathrm{Re}}\frac{\partial u}{\partial x}\right)-\frac{\partial}{\partial y}\left(\frac{1}{\mathrm{Re}}\left(\frac{\partial u}{\partial y}+\frac{\partial v}{\partial x}\right)\right)=0 \qquad (3.31)$$

$$u\frac{\partial v}{\partial x}+v\frac{\partial v}{\partial y}+\frac{\partial P}{\partial y}-\frac{\partial}{\partial y}\left(\frac{2}{\mathrm{Re}}\frac{\partial v}{\partial y}\right)-\frac{\partial}{\partial x}\left(\frac{1}{\mathrm{Re}}\left(\frac{\partial u}{\partial y}+\frac{\partial v}{\partial x}\right)\right)=0$$

To cast the second order system into first order system, we introduce velocity gradients,

$$\frac{\partial u}{\partial x}=u_1, \qquad \frac{\partial u}{\partial y}=u_2, \qquad \frac{\partial v}{\partial x}=u_3, \qquad \frac{\partial v}{\partial y}=u_4, \qquad (3.32)$$

M.D. Gunzburger [19] proposed and iterative penalty method

$$P^k = P^{k-1}-\gamma(\nabla.u) \qquad (3.33)$$

where, k is the nonlinear iteration number. Using iterative penalty method results in a matrix with smaller penalty parameter as the value of the conditioning number needed to enforce the continuity constraint is equal to the square of the parameter needed in the non-iterative method.

In this model we use iterated penalty method in conjunction with finite element discretization. We eliminate pressure and sought solution for velocity field. The model is developed for the velocity gradient based equivalent first order system:

$$u\frac{\partial u}{\partial x}+v\frac{\partial u}{\partial y}-\lambda\frac{\partial}{\partial x}(u_1+u_4)-\frac{\partial}{\partial x}\left(\frac{2}{\mathrm{Re}}u_1\right)-\frac{\partial}{\partial y}\left(\frac{1}{\mathrm{Re}}(u_2+u_3)\right)=0$$

$$u\frac{\partial v}{\partial x}+v\frac{\partial v}{\partial y}-\lambda\frac{\partial}{\partial y}(u_1+u_4)-\frac{\partial}{\partial y}\left(\frac{2}{\mathrm{Re}}u_4\right)-\frac{\partial}{\partial x}\left(\frac{1}{\mathrm{Re}}(u_2+u_3)\right)=0 \qquad (3.34)$$

$$\frac{\partial u}{\partial x}=u_1, \qquad \frac{\partial u}{\partial y}=u_2, \qquad \frac{\partial v}{\partial x}=u_3, \qquad \frac{\partial v}{\partial y}=u_4,$$

where Re=$\rho U_0 L/\mu$ is the Reynolds number.

Let u^h, v^h , u_1^h, u_2^h, u_3^h and u_4^h represent the finite element approximation to the true solution (u, v , u_1, u_2, u_3, u_4). To develop the least-squares finite element model we define the least-squares functional of the residuals over a typical element Ω^e:

$$I^e = \tfrac{1}{2}\int_{\Omega^e}\left(R_1^2+R_2^2+R_3^2+R_4^2+R_5^2+R_6^2\right)dxdy$$

where,

$$R_1 = u^h\frac{\partial u^h}{\partial x}+v^h\frac{\partial u^h}{\partial y}-\lambda\frac{\partial}{\partial x}\left(u_1{}^h+u_4{}^h\right)-\frac{\partial}{\partial x}\left(\frac{2}{\mathrm{Re}}u_1{}^h\right)-\frac{\partial}{\partial y}\left(\frac{1}{\mathrm{Re}}\left(u_2{}^h+u_3{}^h\right)\right) \qquad (3.35)$$

$$R_2 = u^h\frac{\partial v^h}{\partial x}+v^h\frac{\partial v^h}{\partial y}-\lambda\frac{\partial}{\partial y}\left(u_1{}^h+u_4{}^h\right)-\frac{\partial}{\partial y}\left(\frac{2}{\mathrm{Re}}u_4{}^h\right)-\frac{\partial}{\partial x}\left(\frac{1}{\mathrm{Re}}\left(u_2{}^h+u_3{}^h\right)\right)$$

$$R_3=\frac{\partial u^h}{\partial x}-u_1^h, \qquad R_4=\frac{\partial u^h}{\partial y}-u_2^h, \qquad R_5=\frac{\partial v^h}{\partial x}-u_3^h, \qquad R_6=\frac{\partial u^h}{\partial x}-u_4^h,$$

Same order approximation is used for all the primary variables. The field variables are written in the form:

$$u^h(x,y)=\sum_{i=1}^{N}\psi_i(x,y)u^i, \qquad v^h(x,y)=\sum_{i=1}^{N}\psi_i(x,y)v^i,$$

$$u_1{}^h(x,y)=\sum_{i=1}^{N}\Psi_i(x,y)u_1{}^i, \qquad u_2{}^h(x,y)=\sum_{i=1}^{N}\Psi_i(x,y)u_2{}^i,$$

$$u_3{}^h(x,y)=\sum_{i=1}^{N}\psi_i(x,y)u_3{}^i, \qquad u_4{}^h(x,y)=\sum_{i=1}^{N}\psi_i(x,y)u_4{}^h,$$

where, ψ_i are the Lagrange family of interpolation functions and $u^i, v^i, u_1^i, u_2^i, u_3^i, u_4^i$ being the nodal values of $u^h, v^h, u_1^h, u_2^h, u_3^h, u_4^h$.

To minimize the least-square functional, we have to differentiate I^e with respect to nodal of velocities and velocity gradients

$$\delta I^e = \frac{\partial I^e}{\partial u}\delta u + \frac{\partial I^e}{\partial v}\delta v + \frac{\partial I^e}{\partial u_1}\delta u_1 + \frac{\partial I^e}{\partial u_2}\delta u_2 + \frac{\partial I^e}{\partial u_3}\delta u_3 + \frac{\partial I^e}{\partial u_4}\delta u_4$$

Setting the first variation of the least square functional, we get six sets of N equations each over a typical element

$$\frac{\partial I^e}{\partial u^i} = 0, \quad \frac{\partial I^e}{\partial v^i} = 0, \quad \frac{\partial I^e}{\partial u_1^i} = 0, \quad \frac{\partial I^e}{\partial u_2^i} = 0, \quad \frac{\partial I^e}{\partial u_3^i} = 0, \quad \frac{\partial I^e}{\partial u_4^i} = 0,$$

For *i=1,2,……N*. The resulting finite element equations are given by

$$\left[K^e\left(U^e\right)\right]\left\{U^e\right\} = \left\{F^e\right\} \tag{3.36}$$

$$= \begin{bmatrix} K_{ij}^{11} & K_{ij}^{12} & K_{ij}^{13} & K_{ij}^{14} & K_{ij}^{15} & K_{ij}^{16} \\ K_{ij}^{21} & K_{ij}^{22} & K_{ij}^{23} & K_{ij}^{24} & K_{ij}^{25} & K_{ij}^{26} \\ K_{ij}^{31} & K_{ij}^{32} & K_{ij}^{33} & K_{ij}^{34} & K_{ij}^{35} & K_{ij}^{36} \\ K_{ij}^{41} & K_{ij}^{42} & K_{ij}^{43} & K_{ij}^{44} & K_{ij}^{45} & K_{ij}^{46} \\ K_{ij}^{51} & K_{ij}^{52} & K_{ij}^{53} & K_{ij}^{54} & K_{ij}^{55} & K_{ij}^{56} \\ K_{ij}^{61} & K_{ij}^{62} & K_{ij}^{63} & K_{ij}^{64} & K_{ij}^{65} & K_{ij}^{66} \end{bmatrix} \begin{Bmatrix} \{u_j\} \\ \{v_j\} \\ \{u_{1j}\} \\ \{u_{2j}\} \\ \{u_{3_j}\} \\ \{u_{4j}\} \end{Bmatrix} = \begin{Bmatrix} \{F^1\} \\ \{F^2\} \\ \{F^3\} \\ \{F^4\} \\ \{F^5\} \\ \{F^6\} \end{Bmatrix}$$

where,

$$K_{ij}^{11} = \int_{\Omega^e} \left\{ \left(\frac{\partial \mathrm{u}}{\partial \mathrm{x}}\psi_{\mathrm{i}} + u\frac{\partial \psi_i}{\partial x} + v\frac{\partial \psi_i}{\partial y} \right)\left(u\frac{\partial \psi_j}{\partial x} + v\frac{\partial \psi_j}{\partial y} \right) + \frac{\partial \psi_i}{\partial x}\frac{\partial \psi_j}{\partial x} + \frac{\partial \psi_i}{\partial y}\frac{\partial \psi_j}{\partial y} \right\} dxdy$$

$$K_{ij}^{12} = \int_{\Omega^e} \left(\frac{\partial v}{\partial x}\psi_i \right)\left(u\frac{\partial \psi_j}{\partial x} + v\frac{\partial \psi_j}{\partial y} \right) dxdy$$

$$K_{ij}^{13}=\int_{\Omega^e}\left\{\left(\frac{\partial \mathrm{u}}{\partial \mathrm{x}}\psi_{\mathrm{i}}+u\frac{\partial \psi_i}{\partial x}+v\frac{\partial \psi_i}{\partial y}\right)\left(-\gamma\frac{\partial \psi_j}{\partial x}-\frac{2}{\mathrm{Re}}\frac{\partial \psi_j}{\partial x}\right)+\left(\frac{\partial v}{\partial x}\psi_i\right)\left(-\gamma\frac{\partial \psi_j}{\partial y}\right)-\frac{\partial \psi_i}{\partial x}\psi_j\right\}dxdy$$

$$K_{ij}^{14}=\int_{\Omega^e}\left\{\left(\frac{\partial \mathrm{u}}{\partial \mathrm{x}}\psi_{\mathrm{i}}+u\frac{\partial \psi_i}{\partial x}+v\frac{\partial \psi_i}{\partial y}\right)\left(-\frac{1}{\mathrm{Re}}\frac{\partial \psi_j}{\partial y}\right)+\left(\frac{\partial v}{\partial x}\psi_i\right)\left(-\frac{1}{\mathrm{Re}}\frac{\partial \psi_j}{\partial x}\right)-\frac{\partial \psi_i}{\partial y}\psi_j\right\}dxdy$$

$$K_{ij}^{15}=\int_{\Omega^e}\left\{\left(\frac{\partial \mathrm{u}}{\partial \mathrm{x}}\psi_{\mathrm{i}}+u\frac{\partial \psi_i}{\partial x}+v\frac{\partial \psi_i}{\partial y}\right)\left(-\frac{1}{\mathrm{Re}}\frac{\partial \psi_j}{\partial y}\right)+\left(\frac{\partial v}{\partial x}\psi_i\right)\left(-\frac{1}{\mathrm{Re}}\frac{\partial \psi_j}{\partial x}\right)\right\}dxdy$$

$$K_{ij}^{16}=\int_{\Omega^e}\left\{\left(\frac{\partial \mathrm{u}}{\partial \mathrm{x}}\psi_{\mathrm{i}}+u\frac{\partial \psi_i}{\partial x}+v\frac{\partial \psi_i}{\partial y}\right)\left(-\gamma\frac{\partial \psi_j}{\partial x}\right)+\left(\frac{\partial v}{\partial x}\psi_i\right)\left(-\gamma\frac{\partial \psi_j}{\partial y}-\frac{2}{\mathrm{Re}}\frac{\partial \psi_j}{\partial y}\right)\right\}dxdy$$

$$K_{ij}^{21}=\int_{\Omega^e}\left(\frac{\partial u}{\partial y}\Psi_i\right)\left(u\frac{\partial \Psi_j}{\partial x}+v\frac{\partial \Psi_j}{\partial y}\right)dxdy$$

$$K_{ij}^{22}=\int_{\Omega^e}\left\{\left(\frac{\partial \mathrm{v}}{\partial y}\psi_{\mathrm{i}}+u\frac{\partial \psi_i}{\partial x}+v\frac{\partial \psi_i}{\partial y}\right)\left(u\frac{\partial \psi_j}{\partial x}+v\frac{\partial \psi_j}{\partial y}\right)+\frac{\partial \psi_i}{\partial x}\frac{\partial \psi_j}{\partial x}+\frac{\partial \psi_i}{\partial y}\frac{\partial \psi_j}{\partial y}\right\}dxdy$$

$$K_{ij}^{23}=\int_{\Omega^e}\left\{\left(\frac{\partial u}{\partial y}\psi_i\right)\left(-\gamma\frac{\partial \psi_j}{\partial x}-\frac{2}{\mathrm{Re}}\frac{\partial \psi_j}{\partial x}\right)+\left(\frac{\partial \mathrm{v}}{\partial y}\psi_{\mathrm{i}}+u\frac{\partial \psi_i}{\partial x}+v\frac{\partial \psi_i}{\partial y}\right)\left(-\gamma\frac{\partial \psi_j}{\partial y}\right)\right\}dxdy$$

$$K_{ij}^{24}=\int_{\Omega^e}\left\{\left(\frac{\partial u}{\partial y}\Psi_i\right)\left(-\frac{1}{\mathrm{Re}}\frac{\partial \Psi_j}{\partial y}\right)+\left(\frac{\partial \mathrm{v}}{\partial y}\Psi_{\mathrm{i}}+u\frac{\partial \Psi_i}{\partial x}+v\frac{\partial \Psi_i}{\partial y}\right)\left(-\frac{1}{\mathrm{Re}}\frac{\partial \Psi_j}{\partial x}\right)\right\}dxdy$$

$$K_{ij}^{25}=\int_{\Omega^e}\left\{\left(\frac{\partial u}{\partial y}\Psi_i\right)\left(-\frac{1}{\mathrm{Re}}\frac{\partial \Psi_j}{\partial y}\right)+\left(\frac{\partial \mathrm{v}}{\partial y}\Psi_{\mathrm{i}}+u\frac{\partial \Psi_i}{\partial x}+v\frac{\partial \Psi_i}{\partial y}\right)\left(-\frac{1}{\mathrm{Re}}\frac{\partial \Psi_j}{\partial x}\right)-\frac{\partial \Psi_i}{\partial x}\Psi_j\right\}dxdy$$

$$K_{ij}^{26}=\int_{\Omega^e}\left\{\left(\frac{\partial u}{\partial y}\Psi_i\right)\left(-\gamma\frac{\partial \Psi_j}{\partial x}\right)+\left(\frac{\partial \mathrm{v}}{\partial y}\Psi_{\mathrm{i}}+u\frac{\partial \Psi_i}{\partial x}+v\frac{\partial \Psi_i}{\partial y}\right)\left(-\gamma\frac{\partial \Psi_j}{\partial y}-\frac{2}{\mathrm{Re}}\frac{\partial \Psi_j}{\partial y}\right)-\frac{\partial \Psi_i}{\partial y}\Psi_j\right\}dxdy$$

$$K_{ij}^{31}=\int_{\Omega^e}\left\{\left(-\gamma\frac{\partial \Psi_i}{\partial x}-\frac{2}{\mathrm{Re}}\frac{\partial \Psi_i}{\partial x}\right)\left(u\frac{\partial \Psi_j}{\partial x}+v\frac{\partial \Psi_j}{\partial y}\right)-\Psi_i\frac{\partial \Psi_j}{\partial x}\right\}dxdy$$

$$K_{ij}^{32} = \int_{\Omega^e} \left(-\gamma \frac{\partial \Psi_i}{\partial y} \right) \left(u \frac{\partial \Psi_j}{\partial x} + v \frac{\partial \Psi_j}{\partial y} \right) dxdy$$

$$K_{ij}^{33} = \int_{\Omega^e} \left\{ \left(-\gamma \frac{\partial \Psi_i}{\partial x} - \frac{2}{\mathrm{Re}} \frac{\partial \Psi_i}{\partial x} \right) \left(-\gamma \frac{\partial \Psi_j}{\partial x} - \frac{2}{\mathrm{Re}} \frac{\partial \Psi_j}{\partial x} \right) + \left(-\gamma \frac{\partial \Psi_i}{\partial y} \right) \left(-\gamma \frac{\partial \Psi_j}{\partial y} \right) + \Psi_i \Psi_j \right\} dxdy$$

$$K_{ij}^{34} = \int_{\Omega^e} \left\{ \left(-\gamma \frac{\partial \Psi_i}{\partial x} - \frac{2}{\mathrm{Re}} \frac{\partial \Psi_i}{\partial x} \right) \left(-\frac{1}{\mathrm{Re}} \frac{\partial \Psi_j}{\partial y} \right) + \left(-\gamma \frac{\partial \Psi_i}{\partial y} \right) \left(-\frac{1}{\mathrm{Re}} \frac{\partial \Psi_j}{\partial x} \right) \right\} dxdy$$

$$K_{ij}^{35} = \int_{\Omega^e} \left\{ \left(-\gamma \frac{\partial \Psi_i}{\partial x} - \frac{2}{\mathrm{Re}} \frac{\partial \Psi_i}{\partial x} \right) \left(-\frac{1}{\mathrm{Re}} \frac{\partial \Psi_j}{\partial y} \right) + \left(-\gamma \frac{\partial \Psi_i}{\partial y} \right) \left(-\frac{1}{\mathrm{Re}} \frac{\partial \Psi_j}{\partial x} \right) \right\} dxdy$$

$$K_{ij}^{36} = \int_{\Omega^e} \left\{ \left(-\gamma \frac{\partial \Psi_i}{\partial x} - \frac{2}{\mathrm{Re}} \frac{\partial \Psi_i}{\partial x} \right) \left(-\gamma \frac{\partial \Psi_j}{\partial x} \right) + \left(-\gamma \frac{\partial \Psi_i}{\partial y} \right) \left(-\gamma \frac{\partial \Psi_j}{\partial y} - \frac{2}{\mathrm{Re}} \frac{\partial \Psi_j}{\partial y} \right) \right\} dxdy$$

$$K_{ij}^{41} = \int_{\Omega^e} \left\{ \left(-\frac{1}{\mathrm{Re}} \frac{\partial \Psi_i}{\partial y} \right) \left(u \frac{\partial \Psi_j}{\partial x} + v \frac{\partial \Psi_j}{\partial y} \right) - \Psi_i \frac{\partial \Psi_j}{\partial y} \right\} dxdy$$

$$K_{ij}^{42} = \int_{\Omega^e} \left(-\frac{1}{\mathrm{Re}} \frac{\partial \Psi_i}{\partial x} \right) \left(u \frac{\partial \Psi_j}{\partial x} + v \frac{\partial \Psi_j}{\partial y} \right) dxdy$$

$$K_{ij}^{43} = \int_{\Omega^e} \left\{ \left(-\frac{1}{\mathrm{Re}} \frac{\partial \Psi_i}{\partial y} \right) \left(-\gamma \frac{\partial \Psi_j}{\partial x} - \frac{2}{\mathrm{Re}} \frac{\partial \Psi_j}{\partial x} \right) + \left(-\frac{1}{\mathrm{Re}} \frac{\partial \Psi_i}{\partial x} \right) \left(-\gamma \frac{\partial \Psi_j}{\partial y} \right) \right\} dxdy$$

$$K_{ij}^{44} = \int_{\Omega^e} \left\{ \left(-\frac{1}{\mathrm{Re}} \frac{\partial \Psi_i}{\partial y} \right) \left(-\frac{1}{\mathrm{Re}} \frac{\partial \Psi_j}{\partial y} \right) + \left(-\frac{1}{\mathrm{Re}} \frac{\partial \Psi_i}{\partial x} \right) \left(-\frac{1}{\mathrm{Re}} \frac{\partial \Psi_j}{\partial x} \right) + \Psi_i \Psi_j \right\} dxdy$$

$$K_{ij}^{45} = \int_{\Omega^e} \left\{ \left(-\frac{1}{\mathrm{Re}} \frac{\partial \Psi_i}{\partial y} \right) \left(-\frac{1}{\mathrm{Re}} \frac{\partial \Psi_j}{\partial y} \right) + \left(-\frac{1}{\mathrm{Re}} \frac{\partial \Psi_i}{\partial x} \right) \left(-\frac{1}{\mathrm{Re}} \frac{\partial \Psi_j}{\partial x} \right) \right\} dxdy$$

$$K_{ij}^{46} = \int_{\Omega^e} \left\{ \left(-\frac{1}{\mathrm{Re}} \frac{\partial \Psi_i}{\partial y} \right) \left(-\gamma \frac{\partial \Psi_j}{\partial x} \right) + \left(-\frac{1}{\mathrm{Re}} \frac{\partial \Psi_i}{\partial x} \right) \left(-\gamma \frac{\partial \Psi_j}{\partial y} - \frac{2}{\mathrm{Re}} \frac{\partial \Psi_j}{\partial y} \right) \right\} dxdy$$

$$K_{ij}^{51} = \int_{\Omega^e} \left(-\frac{1}{\mathrm{Re}} \frac{\partial \Psi_i}{\partial y} \right) \left(u \frac{\partial \Psi_j}{\partial x} + v \frac{\partial \Psi_j}{\partial y} \right) dxdy$$

$$K_{ij}^{52} = \int_{\Omega^e} \left\{ \left(-\frac{1}{\mathrm{Re}} \frac{\partial \Psi_i}{\partial x} \right) \left(u \frac{\partial \Psi_j}{\partial x} + v \frac{\partial \Psi_j}{\partial y} \right) - \Psi_i \frac{\partial \Psi_j}{\partial x} \right\} dxdy$$

$$K_{ij}^{53} = \int_{\Omega^e} \left\{ \left(-\frac{1}{\mathrm{Re}} \frac{\partial \Psi_i}{\partial y} \right) \left(-\gamma \frac{\partial \Psi_j}{\partial x} - \frac{2}{\mathrm{Re}} \frac{\partial \Psi_j}{\partial x} \right) + \left(-\frac{1}{\mathrm{Re}} \frac{\partial \Psi_i}{\partial x} \right) \left(-\gamma \frac{\partial \Psi_j}{\partial y} \right) \right\} dxdy$$

$$K_{ij}^{54} = \int_{\Omega^e} \left\{ \left(-\frac{1}{\mathrm{Re}} \frac{\partial \Psi_i}{\partial y} \right) \left(-\frac{1}{\mathrm{Re}} \frac{\partial \Psi_j}{\partial y} \right) + \left(-\frac{1}{\mathrm{Re}} \frac{\partial \Psi_i}{\partial x} \right) \left(-\frac{1}{\mathrm{Re}} \frac{\partial \Psi_j}{\partial x} \right) \right\} dxdy$$

$$K_{ij}^{55} = \int_{\Omega^e} \left\{ \left(-\frac{1}{\mathrm{Re}} \frac{\partial \Psi_i}{\partial y} \right) \left(-\frac{1}{\mathrm{Re}} \frac{\partial \Psi_j}{\partial y} \right) + \left(-\frac{1}{\mathrm{Re}} \frac{\partial \Psi_i}{\partial x} \right) \left(-\frac{1}{\mathrm{Re}} \frac{\partial \Psi_j}{\partial x} \right) + \Psi_i \Psi_j \right\} dxdy$$

$$K_{ij}^{56} = \int_{\Omega^e} \left\{ \left(-\frac{1}{\mathrm{Re}} \frac{\partial \Psi_i}{\partial y} \right) \left(-\gamma \frac{\partial \Psi_j}{\partial x} \right) + \left(-\frac{1}{\mathrm{Re}} \frac{\partial \Psi_i}{\partial x} \right) \left(-\gamma \frac{\partial \Psi_j}{\partial y} - \frac{2}{\mathrm{Re}} \frac{\partial \Psi_j}{\partial y} \right) \right\} dxdy$$

$$K_{ij}^{61} = \int_{\Omega^e} \left(-\gamma \frac{\partial \Psi_i}{\partial x} \right) \left(u \frac{\partial \Psi_j}{\partial x} + v \frac{\partial \Psi_j}{\partial y} \right) dxdy$$

$$K_{ij}^{62} = \int_{\Omega^e} \left\{ \left(-\gamma \frac{\partial \Psi_i}{\partial y} - \frac{2}{\mathrm{Re}} \frac{\partial \Psi_i}{\partial y} \right) \left(u \frac{\partial \Psi_j}{\partial x} + v \frac{\partial \Psi_j}{\partial y} \right) - \Psi_i \frac{\partial \Psi_j}{\partial y} \right\} dxdy$$

$$K_{ij}^{63} = \int_{\Omega^e} \left\{ \left(-\gamma \frac{\partial \Psi_i}{\partial x} \right) \left(-\gamma \frac{\partial \Psi_j}{\partial x} - \frac{2}{\mathrm{Re}} \frac{\partial \Psi_j}{\partial x} \right) + \left(-\gamma \frac{\partial \Psi_i}{\partial y} - \frac{2}{\mathrm{Re}} \frac{\partial \Psi_i}{\partial y} \right) \left(-\gamma \frac{\partial \Psi_j}{\partial y} \right) \right\} dxdy$$

$$K_{ij}^{64} = \int_{\Omega^e} \left\{ \left(-\gamma \frac{\partial \Psi_i}{\partial x} \right) \left(-\frac{1}{\mathrm{Re}} \frac{\partial \Psi_j}{\partial y} \right) + \left(-\gamma \frac{\partial \Psi_i}{\partial y} - \frac{2}{\mathrm{Re}} \frac{\partial \Psi_i}{\partial y} \right) \left(-\frac{1}{\mathrm{Re}} \frac{\partial \Psi_j}{\partial x} \right) \right\} dxdy$$

$$K_{ij}^{65} = \int_{\Omega^e} \left\{ \left(-\gamma \frac{\partial \Psi_i}{\partial x} \right) \left(-\frac{1}{\mathrm{Re}} \frac{\partial \Psi_j}{\partial y} \right) + \left(-\gamma \frac{\partial \Psi_i}{\partial y} - \frac{2}{\mathrm{Re}} \frac{\partial \Psi_i}{\partial y} \right) \left(-\frac{1}{\mathrm{Re}} \frac{\partial \Psi_j}{\partial x} \right) \right\} dxdy$$

$$K_{ij}^{66} = \int_{\Omega^e} \left\{ \left(-\gamma \frac{\partial \Psi_i}{\partial x} \right) \left(-\gamma \frac{\partial \Psi_j}{\partial x} \right) + \left(-\gamma \frac{\partial \Psi_i}{\partial y} - \frac{2}{\mathrm{Re}} \frac{\partial \Psi_i}{\partial y} \right) \left(-\gamma \frac{\partial \Psi_j}{\partial y} - \frac{2}{\mathrm{Re}} \frac{\partial \Psi_j}{\partial y} \right) + \Psi_i \Psi_j \right\} dxdy$$

$$F_i^1 = \int_{\Omega^e} \left\{ \left(\frac{\partial \mathrm{u}}{\partial \mathrm{x}} \psi_{\mathrm{i}} + u \frac{\partial \psi_i}{\partial x} + v \frac{\partial \psi_i}{\partial y} \right) \left(f_x - \frac{\partial P}{\partial x} \right) + \left(\frac{\partial v}{\partial x} \psi_i \right) \left(f_y - \frac{\partial P}{\partial y} \right) \right\} dxdy$$

$$F_i^2 = \int_{\Omega^e} \left\{ \left(\frac{\partial u}{\partial y} \psi_i \right) \left(f_x - \frac{\partial P}{\partial x} \right) + \left(\frac{\partial \mathrm{v}}{\partial y} \psi_{\mathrm{i}} + u \frac{\partial \psi_i}{\partial x} + v \frac{\partial \psi_i}{\partial y} \right) \left(f_y - \frac{\partial P}{\partial y} \right) \right\} dxdy$$

$$F_i^3 = \int_{\Omega^e} \left\{ \left(-\gamma \frac{\partial \Psi_i}{\partial x} - \frac{2}{\mathrm{Re}} \frac{\partial \Psi_i}{\partial x} \right) \left(f_x - \frac{\partial P}{\partial x} \right) + \left(-\gamma \frac{\partial \Psi_i}{\partial y} \right) \left(f_y - \frac{\partial P}{\partial y} \right) \right\} dxdy$$

$$F_i^4 = \int_{\Omega^e} \left\{ \left(-\frac{1}{\mathrm{Re}} \frac{\partial \Psi_i}{\partial y} \right) \left(f_x - \frac{\partial P}{\partial x} \right) + \left(-\frac{1}{\mathrm{Re}} \frac{\partial \Psi_i}{\partial x} \right) \left(f_y - \frac{\partial P}{\partial y} \right) \right\} dxdy$$

$$F_i^5 = \int_{\Omega^e} \left\{ \left(-\frac{1}{\mathrm{Re}} \frac{\partial \Psi_i}{\partial y} \right) \left(f_x - \frac{\partial P}{\partial x} \right) + \left(-\frac{1}{\mathrm{Re}} \frac{\partial \Psi_i}{\partial x} \right) \left(f_y - \frac{\partial P}{\partial y} \right) \right\} dxdy$$

$$F_i^6 = \int_{\Omega^e} \left\{ \left(-\gamma \frac{\partial \Psi_i}{\partial x} \right) \left(f_x - \frac{\partial P}{\partial x} \right) + \left(-\gamma \frac{\partial \Psi_i}{\partial y} - \frac{2}{\mathrm{Re}} \frac{\partial \Psi_i}{\partial y} \right) \left(f_y - \frac{\partial P}{\partial y} \right) \right\} dxdy \qquad (3.38)$$

3.4.2. Nonlinear Equation Solving Procedures

The algebraic equations we got in matrix form are nonlinear in nature. Iterative methods are used to solve them. The direct iteration technique was used for the present numerical implementation.

3.4.2.1 Direct Iteration Method

The direct method or Picard iteration method is a simple technique.

The nonlinear matrix equation of the form

$$[K(\{U\})]U = \{F\} \tag{3.39}$$

Where, K is the coefficient matrix. For nonlinear equations the coefficient matrix is a function of the unknown. We evaluate the coefficient matrix using an initial guess or the solution from previous iteration. So equation (3.39) is written as

$$\left[K(\{U\})^{n-1}\right]U^{n} = \{F\} \tag{3.40}$$

So we assume that solution vector at (n-1)th iteration is known and evaluate K. Then find solution for the nth iteration using equation (3.40). At the beginning of the iteration the solution vector is guessed. As we are using an estimated vector in equation (3.40), we get a residual.

$$R \equiv \left[K(\{U\})^{n-1}\right]U^{n} - \{F\} \tag{3.41}$$

The iterations are carried on until the following criterion is satisfied

$$\sqrt{\frac{\sum_{I=1}^{N}\left|U_I^{(r)} - U_I^{(r-1)}\right|^2}{\sum_{I=1}^{N}\left|U_I^{(r)}\right|^2}} \le \in$$

where, ϵ is the tolerance. In this study the tolerance was chosen to be 0.01. The flow chart [1] of the direct iteration method is given in the Fig. 3.1 [25].

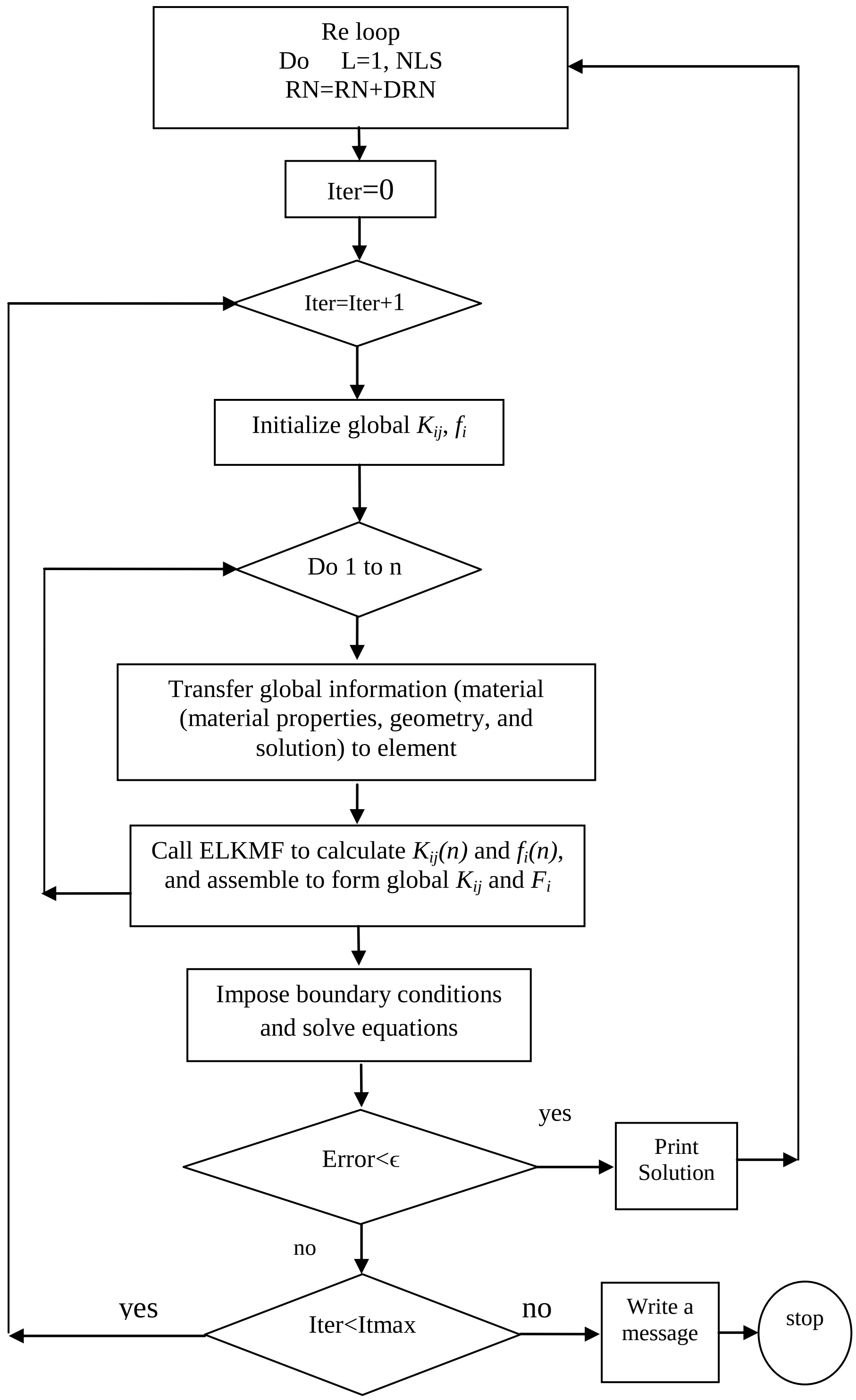

Fig**.** 3.1. A computer flow chart for the nonlinear finite element analysis

3.4.3. Numerical Results

The two-dimensional 'driven cavity' was considered to analyze accuracy and convergence characteristic of the penalty least-square formulation. The boundary conditions for velocities u ,v are shown in the Fig. (3.2)

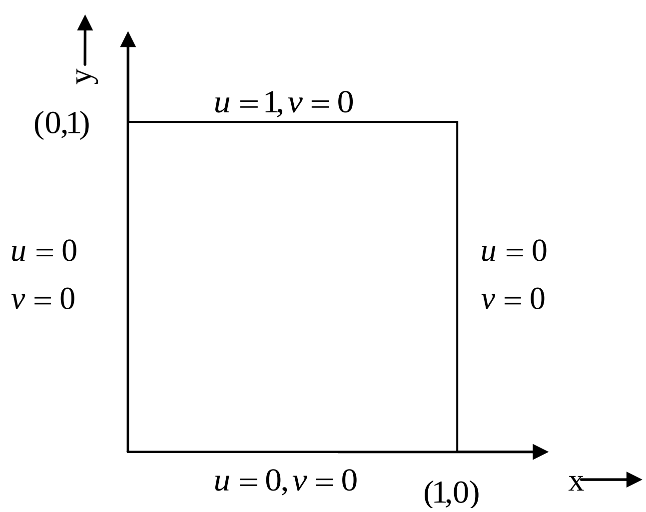

Fig.3.2. Schematic of driven cavity problem

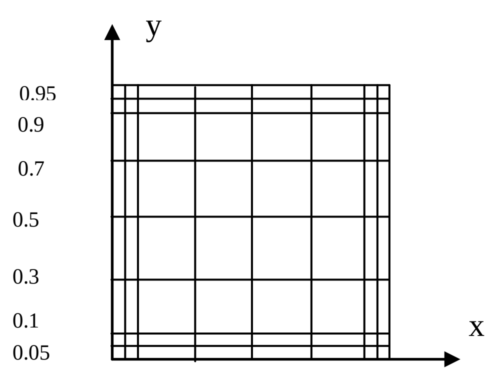

Fig.3.3. Finite element model of driven cavity

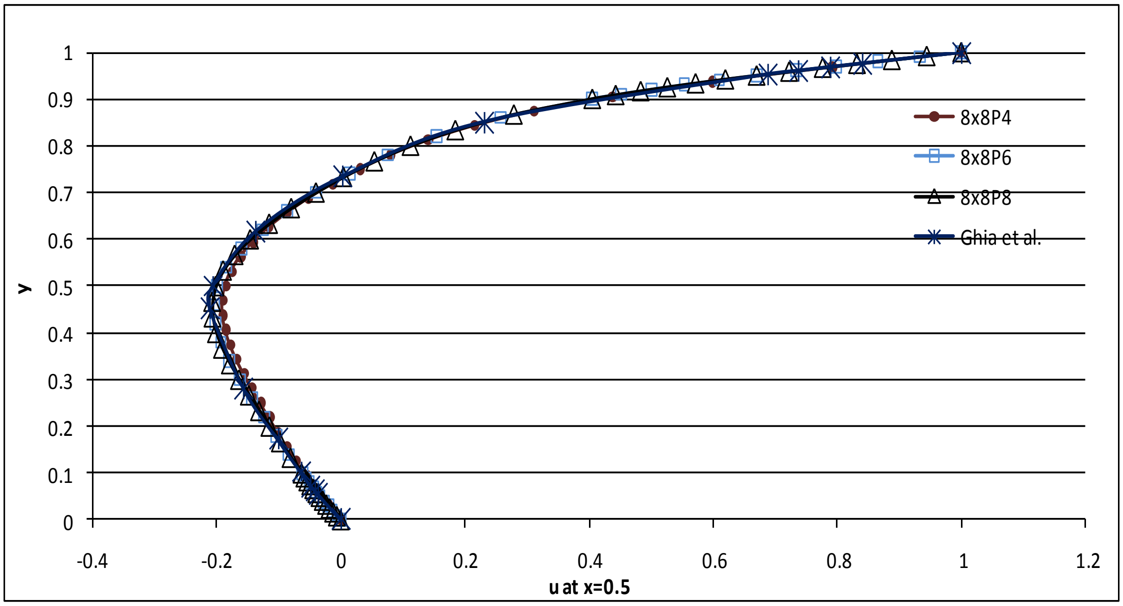

Fig.3.4(a). Plots of u(x=0.5,y) at Re=100

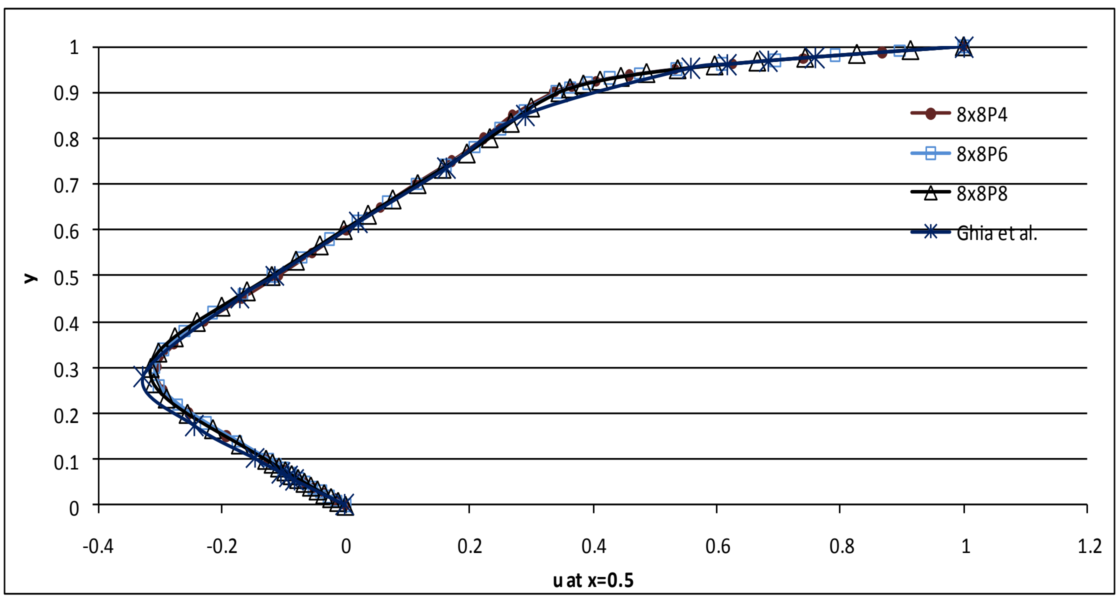

Fig.3.4(b). Plots of u(x=0.5,y) at Re=400

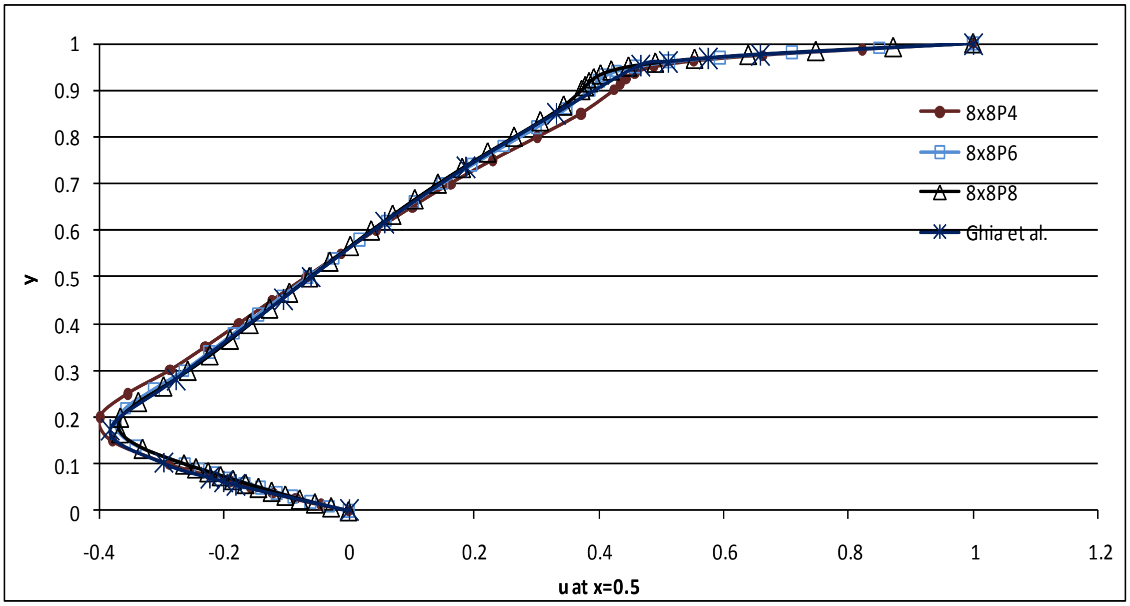

Fig.3.4(c). Plots of u(x=0.5,y) at Re=1000

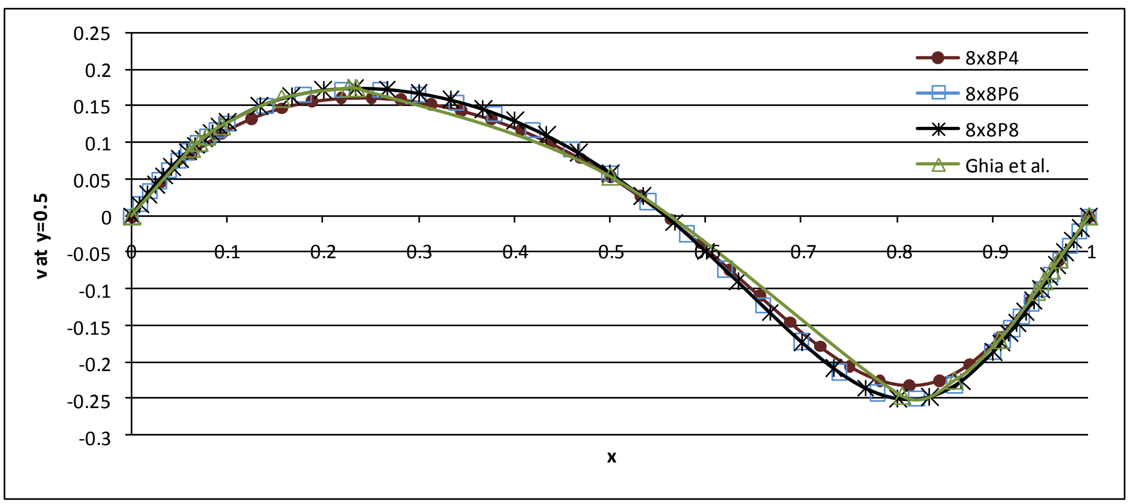

Fig. 3.5(a).Plots of v(x,y=0.5) at Re=100

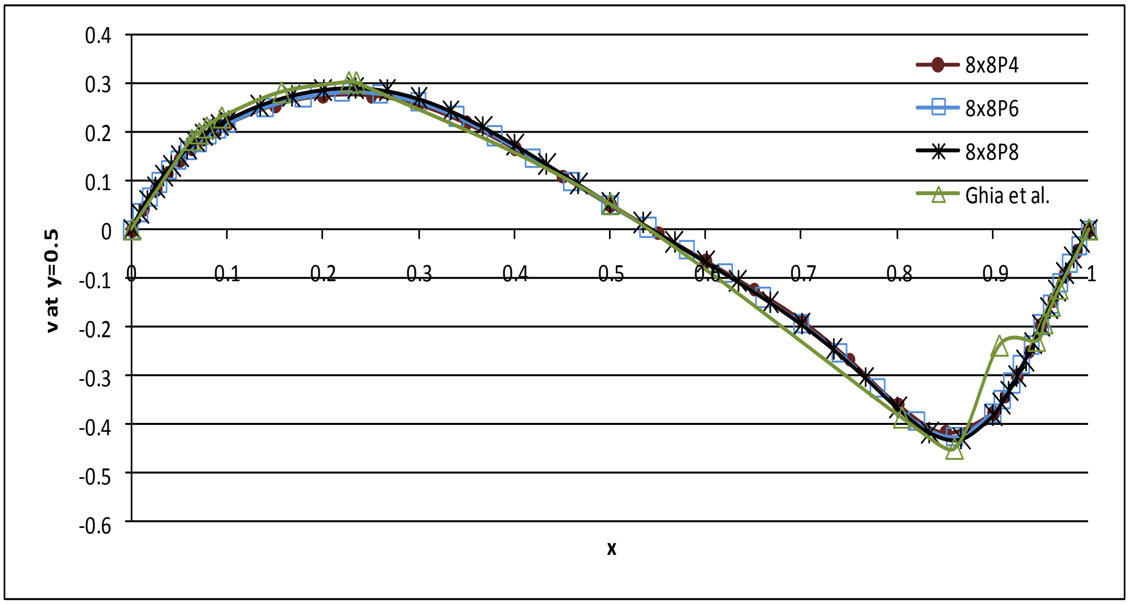

Fig. 3.5(b). Plots of v(x ,y=0.5) at Re=400

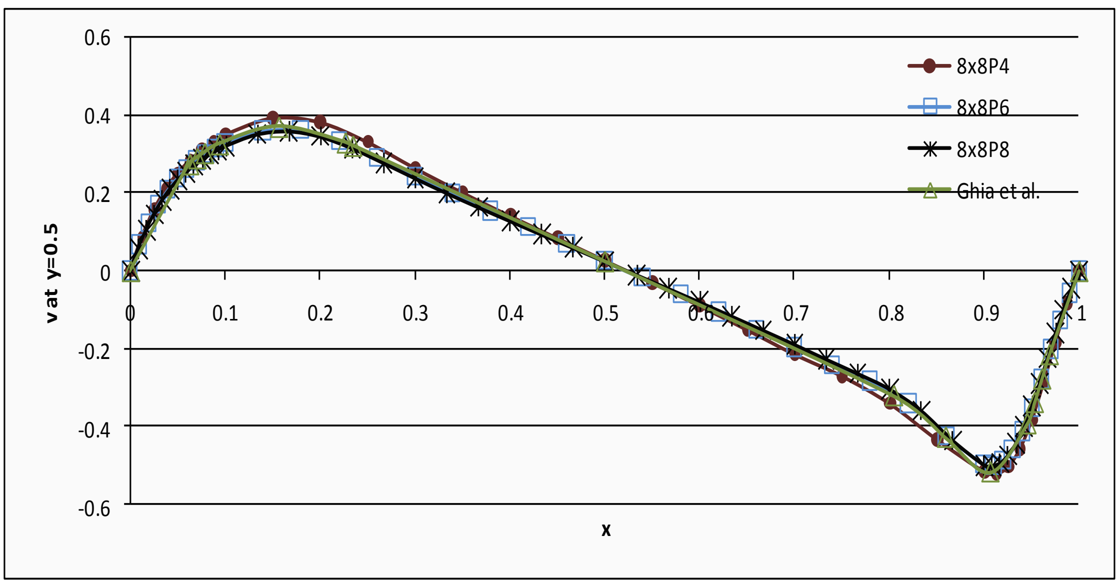

Fig.3.5(c). Plots of v(x ,y=0.5) at Re=1000

Fig. 3.3 shows the 8x8 finely graded mesh used for the numerical analysis. The elements adjacent to the four boundaries of the cavity are 0.05 units. The p-levels in the $\xi-$ and $\eta-$ directions $\left(p_\xi = p_\eta\right)$ were uniformly increased from three to six. The problem was solved using penalty parameter 100. A marching scheme was used, starting with Re=100 and march till Re=1000 with an increment of 100. Direct iteration required less than 5 iterations for a convergence tolerance of 0.01.

The *u*-velocity profiles along the vertical mid-line of the cavity (x=0.5) are shown in Fig. 3.4(a)-3.4(c) and the *v*-velocity profiles along the horizontal mid-line of the cavity (y=0.5) are presented in Fig. 3.5(a)-3.5(c) for Re=100,400 and 1000 respectively. The results reported by Ghia *et al.* [26] are used as a reference. The solutions for u and v show excellent agreement with the reference solution [26].

CHAPTER IV

CONCLUSIONS

The least-squares formulation can be applied to linear as well as nonlinear set of partial differential equations. The method satisfies the criteria desirable in a variational method. Successful application of this method requires that the set of equations be cast into their first order equivalent. This would allow us to use C^0 continuous approximation function for the primary and auxiliary variables.

In chapter II, we presented least square formulations for the Poisson equation. In a conventional model based on weak form Galerkin, fluxes have to be post computed. Higher order polynomial approximation was required to predict the fluxes accurately. Using LSFEM, the fluxes are introduced as auxiliary variables and are predicted accurately with a lower order polynomial approximation. Applying least-square principle directly to the Poisson equation however, needed a very refined mesh to predict results close to the exact solution.

In chapter III, the penalty based least-squares formulation for the viscous, incompressible Navier-Stokes equation was presented. With a penalty parameter as small as 100 accurate results were obtained with this model. It is also a better alternative to the conventional weak form penalty finite element model which requires large values of penalty parameter $\left(10^4\,\mathrm{Re} - 10^{12}\,\mathrm{Re}\right)$. In addition, there is no need to under-integrate the penalty terms of the coefficient matrix. The least-squares model was based on velocity and velocity gradients. Numerical results were presented for the 2D lid-driven cavity flow. The *p*-version of the finite element method showed excellent convergence characteristic.

REFERENCES

[1] J.P. Pontaza, J.N. Reddy, Spectral/*hp* least-squares finite element formulation for the Navier-Stokes equations, J. Comput. Phys. 190 (2003) 523.

[2] J. Franz, M. Kasper, Superconvergent finite element solutions of Laplace and Poisson equation, IEEE Transactions on Magnetics 32 (1996) 643.

[3] P.B. Bochev, M.D. Gunzburger, Finite element methods of least-squares type, SIAM Rev. 40 (1998) 789.

[4] J.F. Polk, P.P. Lynn, A least squares finite element approach to unsteady gas dynamics, Int. J. Numer. Methods Engrg. 12 (1978) 3-10.

[5] M. Becker, The principles and applications of' variational methods, research monograph 27, Massachusetts Institute of Technology Press, Cambridge, MA, 1964.

[6] B.N. Jiang, C.L. Chang, Least-squares finite elements for the Stokes problem, Comput. Methods Appl. Mech. Engrg. 78 (1990) 297-31 1.

[7] P.P. Lynn, S.K. Arya, Use of the least squares criterion in the finite element formulation, Int. J. Numer. Methods Engrg. 6 (1973) 75-88.

[8] J. F. Polk, P. P. Lynn, A least squares finite element approach to unsteady gas dynamics, Int. J. Numer. Methods Engrg. 12 (1978) 3-10.

[9] C.A.J. Fletcher, A primitive variable finite element formulation for inviscid, compressible flow, J. Comput. Phys. 33 (1979) 301-312.

[10] H. Nguyen, J. Reynen, A space-time least-square finite element scheme for advection-diffusion equations, Computer Methods Appl. Mech. Engrg. 42 (1984) 331-342.

[11] Kececioglu, B. Rubinsky, A mixed-variable continuously deforming finite element method for parabolic evolution problems. Part II: The coupled problem of phase-change in porous media, Int. J. Numer. Methods Engrg. 28 (1989) 2609-2634.

[12] P.P. Lynn, Least squares finite element analysis of laminar boundary layer flows, Int. J. Numer. Methods Engrg. 8 (2005) 865-867.

[13] G.F. Carey, B.N. Jiang, Least-squares finite elements for first-order hyperbolic systems, Int. J. Numer. Methods Engrg. 26 (1988) 81-93.

[14] G.J. Fix, M.D. Gunzburger, On least squares approximations to indefinite problems of the mixed type, Int.J. Numer. Methods Engrg. 12 (1978) 453-469.

[15] I. Babuska, O.C. Zienkiewicz, J. Gago, E.R. de A. Oliveira, Accuracy Estimates and Adaptive Refinements in Finite Element Computations, Wiley, New York, 1986.

[16] B.N. Jiang, V. Sonnad, Least-squares solution of incompressible Navier- Stokes equations with the p-version of finite elements, NASA Tech. Mem. 105203, ICOMP-91-14, September 1991.

[17] D. Winterscheidt, K. Surana, *p*- version least squares finite element formulation for two-dimensional incompressible fluid flow, Int. J. Numer. Methods Fluids 18 (1994) 43-69.

[18] B.N. Jiang, The Least-squares Finite Element Method, Springer, Berlin, 1998.

[19] M.D. Gunzburger, Iterated penalty methods for the Stokes and Navier-Stokes equations, in: T.J. Chung, G.R. Karr (Eds.), Finite Element Analysis in Fluids,

Proceedings of the 7th International Conference on Finite Element Methods in Flow Problems, University of Alabama Press (1989) 1040-1045.

[20] J. N. Reddy, An Introduction to the Finite Element Method, 3rd ed., McGraw-Hill, New York, 2006.

[21] R. J. Melosh, Basis of derivation of Matrices for the Direct Stiffness Method, AIAA J. 1 (1963) 1631-1637.

[22] O.C. Zienkiewwicz, Y.K. Cheung, The finite element method for analysis of elastic isotropic and orthotropic slabs, Proceedings of the Institute of Civil Engineers, London, 28 (1964) 471-488.

[23] F.K. Bogner, R.L. Fox, Jr. L.A. Schmidt, The generation of interelement-compatible stiffness and mass matrices by the use of interpolation formulae's, Proceedings of the Conference on Matrix Methods in Structural Mechanics, Air Force Institute of Technology, Wright-Patterson Air Force Base, OH, (1965) 397-443.

[24] D.S. Malkus, T.J.R. Hughes, Mixed finite element methods-reduced and selective integration techniques: a unification of concepts, Comput. Methods Appl. Mech. Engrg. 15 (1978) 63-81.

[25] J.N. Reddy, An Introduction to Nonlinear Finite Element Analysis, Oxford University Press, Oxford, 2004.

[26] U. Ghia, K.N. Ghia, C.T. Shin, High-Re solution for incompressible flow using the Navier-Stokes equations and a multigrid, J. Comput. Phys. 48 (1982) 387-411.

[27] Sebastien Lepaul, A. de Lustract, F. Bouillault, Solving the Poisson's and Schrodinger's equations to calculate the electron states in quantum nanostructures using the Finite Element Method, IEEE Transaction on Magnetics 32 (1996) 1018.

[28] J.N. Reddy, An Introduction to Continuum Mechanics: With Applications, Cambridge University Press, New York, 2008.

[29] J. N. Reddy, D. K. Gartling, The Finite Element Method in Heat Transfer and Fluid Dynamics, 2nd edition, CRC Press, Boca Raton, 2001.

[30] J. N. Reddy, Energy Principles and Variational Methods in Applied Mechanics, 2nd ed., John Wiley, New York, 2002.

[31] C.A.J. Fletcher, Computational Techniques for Fluid Dynamics, Vol. 1, 2nd ed., Springer, 2005.

[32] M. Abramowitz, I.A. Stegun, Handbook of Mathematical Functions, Dover Publications, Inc., 1972.

[33] B.C. Bell, K. Surana, *p*-Version least-squares finite element formulation for two-dimensional non-newtonian isothermal and non-isothermal fluid flow, Int. J. Numer. Methods Fluids 18 (1994) 127-162.

[34] G.G. Gu, M.A. Gennert, Boundary element methods for solving Poisson equations in computer vision problems, Proceedings of the IEEE International Conf. Computer Vision and Pattern Recognition, Maui, HI (1991) 546-551.

[35] B.N. Jiang, L.A. Povinelli, Least-squares finite element method for fluid dynamics,' Comput. Methods in Applied Mech. Engrg. 81 (1990) 13-37.

VITA

Nellie Rajarova was born in Bhubaneswar, India. She received her B.Tech degree from National Institute of Technology, Rourkela in May, 2006. She joined the doctoral program at Texas A&M University as a graduate student in August 2006 and on her way to her Ph.D., graduated with her M.S. in May 2009.

Ms.. Rajarova may be reached at 3123 TAMU, College Station, TX 77843-3123. Her email is: nellie.rajarova@gmail.com.